COMPARATIVE QUANTITATIVE RISK ANALYSIS (QRA) FOR LINAM RANCH GAS PLANT GAS PROCESSING AND REINJECTION OPTIONS

Prepared For
Duke Energy Field Services
370 17th Street, Suite 2500
Denver, Colorado 80202

Prepared By
Quest Consultants Inc.
908 26th Avenue, N.W.
Post Office Box 721387
Norman, Oklahoma 73070-8069
Telephone: 405-329-7475
Telecopy: 405-329-7734

February 1, 2006
06-02-6567

QUEST

T F A R D

QUEST

COMPARATIVE QUANTITATIVE RISK ANALYSIS (QRA) FOR LINAM RANCH GAS PLANT GAS PROCESSING AND REINJECTION OPTIONS

Table of Contents

QUEST

Table of Contents
(Continued)

QUEST

List of Tables

QUEST

SECTION 1
INTRODUCTION

Quest Consultants was retained by Duke Energy Field Services to perform a comparative quantitative risk analysis (QRA) of three proposed acid gas injection options and an expanded sulfur recovery unit at the Linam Ranch gas plant near the town of Hobbs, New Mexico. The pipelines and equipment included in the study was limited to those that transport or process hydrogen sulfide or sulfur dioxide:

- Buckeye natural gas (NG) inlet pipeline
- Eddy County NG inlet pipeline
- Lea/Shell NG inlet pipeline
- Sour gas amine treating unit
- Sulfur recovery unit (SRU)
- Acid gas injection (AGI) option #1 – compression at Linam Ranch gas plant
- Acid gas injection option #2 – compression at Linam Ranch and at AGI wellsite
- Acid gas injection option #3 – compression at AGI wellsite.
- Acid gas injection wellsite

The objective of the study was to compare the level of toxic risk posed by the four proposed project options. The study was divided into three primary tasks. First, determine potential releases that could result in significant hazardous conditions along the pipelines, near the gas plant, and near the injection wellsite. Second, for those potential releases identified, derive a frequency (or probability) of release. Third, using consistent, accepted methodology, combine the potential release consequences with the release frequencies to arrive at a measure of the toxic risk posed to the public. Figure 1-1 illustrates the steps in the QRA procedure required to complete the three primary tasks.

1.1   Hazards Identification

The potential hazards associated with the pipelines, treating, and injection facilities are common to similar processes worldwide, and are a function of the materials being processed, processing systems, procedures used for operating and maintaining the equipment, and hazard detection and mitigation systems provided. The hazards that are likely to exist are identified by the physical and chemical properties of the materials being handled, and the process conditions. For facilities handling flammable and toxic gases, the common hazards are:

- torch fires
- flash fires
- vapor cloud explosions
- toxic gas clouds (fluids containing hydrogen sulfide and sulfur dioxide)

For this study, only toxic hazards were considered since the flammable hazards are common to each project option.

The hazards identification step is discussed in Sections 2 and 3.

QUEST

QUANTITATIVE RISK ANALYSIS STEPS	TOOLS UTILIZED

QUANTITATIVE RISK ANALYSIS STEPS
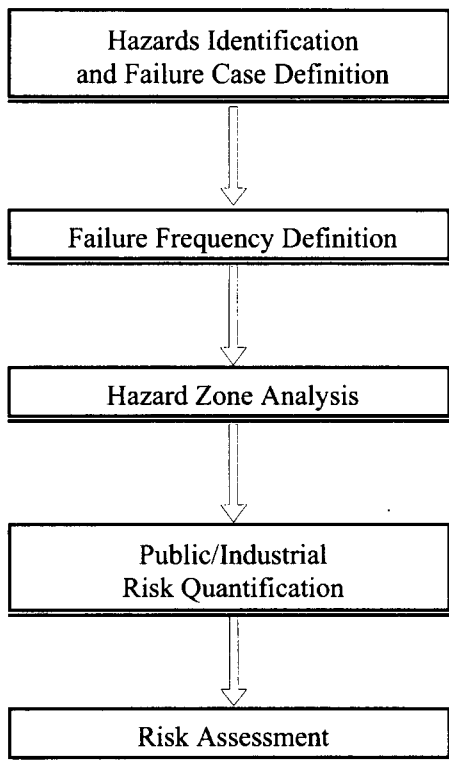
TOOLS UTILIZED

```
┌─────────────────────────┐       • Industrial accident histories
│  Hazards Identification │       • Review of project design information
│ and Failure Case Definition │    • Review of hazard detection and mitigation
└─────────────────────────┘         systems
            │
            ▽
┌─────────────────────────┐       • Single component failure rates
│ Failure Frequency Definition │   • Fault Tree Analysis (FTA)
└─────────────────────────┘
            │
            ▽
┌─────────────────────────┐       • Hazard computation models for fires,
│   Hazard Zone Analysis  │         explosions, and gas clouds
└─────────────────────────┘       • Hazard contours for people
            │
            ▽
┌─────────────────────────┐       • Population distribution near the site
│     Public/Industrial   │       • Local weather conditions
│   Risk Quantification   │       • Local topography
└─────────────────────────┘
            │
            ▽
┌─────────────────────────┐       • Acceptable risk values
│     Risk Assessment     │
└─────────────────────────┘
```

Figure 1-1
Overview of Risk Analysis Methodology

1.2 Failure Case Definition

The potential release sources of process materials or working fluids are determined from a combination of past history of releases from similar facilities and facility-specific information, including Process Flow Diagrams (PFDs), Piping and Instrumentation Diagrams (P&IDs), accident data, and engineering analysis by system safety engineers. Other methods that may be used in selected instances include Failure Modes and Effects Analysis (FMEA) and Hazards and Operability (HAZOP) studies.

This step in the analysis defines the various release sources and conditions of release for each failure case. The release conditions include:

- fluid composition, temperature, and pressure
- release rate and duration
- location and orientation of the release
- type of surface over which released liquid (if any) spreads

The failure case definition step is included in Section 3.

QUEST

1.3   Failure Frequency Definition

The frequency with which a given failure case is expected to occur can be estimated by using a combination of:

- historical experience
- failure rate data on similar types of equipment
- service factors
- engineering judgment

For single component failures (e.g., pipe rupture), the failure frequency can be determined from industrial failure rate data bases. For multiple component failures (e.g., failure of a high pressure alarm and shutdown of a compressor discharge line), Fault Tree Analysis (FTA) techniques can be used. The single component failure rates used in constructing the fault tree are obtained from industrial failure rate data bases. The failure frequency step is included in Section 4.

1.4   Hazard Zone Analysis

The release conditions (e.g., pressure, composition, temperature, hole size, inventory, etc.) from the failure case definitions are then processed, using the best available hazard quantification technology, to produce a set of hazard zones for each failure case. The CANARY by Quest® computer software hazards analysis package is used to produce profiles for the fire, explosion, and toxic hazards associated with the failure case. The models that are used account for:

- release conditions
- ambient weather conditions (wind speed, air temperature, humidity, atmospheric stability)
- effects of the local terrain (diking, vegetation)
- mixture thermodynamics

The hazard zone analysis step is included in Section 3.

1.5   Public/Industrial Risk Quantification

The methodology used in this study follows internationally accepted guidelines and has been successfully employed in QRA studies that have undergone regulatory review in countries worldwide. This methodology is described in Section 5.

The result of the analysis is a prediction of the risk posed by the pipelines, gas treatment facilities, compression equipment, and injection well. Risk may be expressed in several forms (e.g., risk contours, average individual risk, societal risk, etc.). For this analysis, the focus was on the prediction of risk contours for toxic exposure.

1.6   Risk Assessment

Risk indicators enable decision makers (i.e., corporate risk managers or regulatory authorities) to evaluate the risks associated with the three options for acid gas reinjection and the expanded sulfur recovery unit at the Linam Ranch gas plant. Risk contours for the various pipelines and surface facility options can be compared to assist the decision makers in making judgments about the acceptability of the risk associated with the project. Results of the risk analysis and conclusions drawn from this study are presented in Section 6.

QUEST

QUEST

SECTION 2
FACILITY LOCATION, PIPELINE ROUTES, PIPELINE DATA, AND WELL DATA

2.1 Facility Location

The Linam Ranch natural gas processing facility, pipelines, and proposed injection well are located just west of the town of Hobbs, New Mexico. A regional overview is presented in Figure 2-1. The portions of the pipeline system to be evaluated consists of four incoming natural gas pipelines, the amine sour gas sweetening system, the existing sulfur recovery unit, and three proposed systems for reinjecting hydrogen sulfide (H_2S) and carbon dioxide (CO_2). The H_2S/CO_2 gas is to be reinjected at the AGI Linum #1 well site. General characteristics of the system are shown in Figure 2-1; system details are discussed below. The basis of the study is a plant processing rate of 200 million standard cubic feet per day (200 mmscfd).

2.2 Pipeline Routes

2.2.1 Buckeye Pipeline

The Buckeye pipeline feeds into the Linam Ranch gas plant from the northwest. Gas is received at the Linam metering station, where ESD valves, metering, and pig launchers are located. The Buckeye pipeline originates northwest of the Linam plant, runs southeast, and turns south, crossing State Highway 62 (Carlsbad Highway) just before entering the gas plant. The anticipated gas flow rate through the 10-inch Buckeye pipeline is 57 mmscfd.

2.2.2 Eddy Pipeline

The 12-inch Eddy pipeline feeds into the Linam Ranch gas plant from the west-northwest. Gas is received at the Linam metering station. The Eddy pipeline runs east-southeast, then turns south, crossing State Highway 62 (Carlsbad Highway) just before entering the gas plant. The Eddy pipeline will have an average gas flow rate of 95 mmscfd.

2.2.3 Shell/Lea Pipeline

The 12-inch Shell/Lea pipeline feeds into the Linam Ranch gas plant from the south. The inlet gas flow is combined from the Lea County pipeline, which is currently shutdown, and the Shell pipeline. Gas is received at the Linam metering station. The Shell pipeline runs east before joining with the abandoned Lea County pipeline running north into the plant. The anticipated gas flow rate through the Shell/Lea pipeline is 48 mmscfd.

QUEST
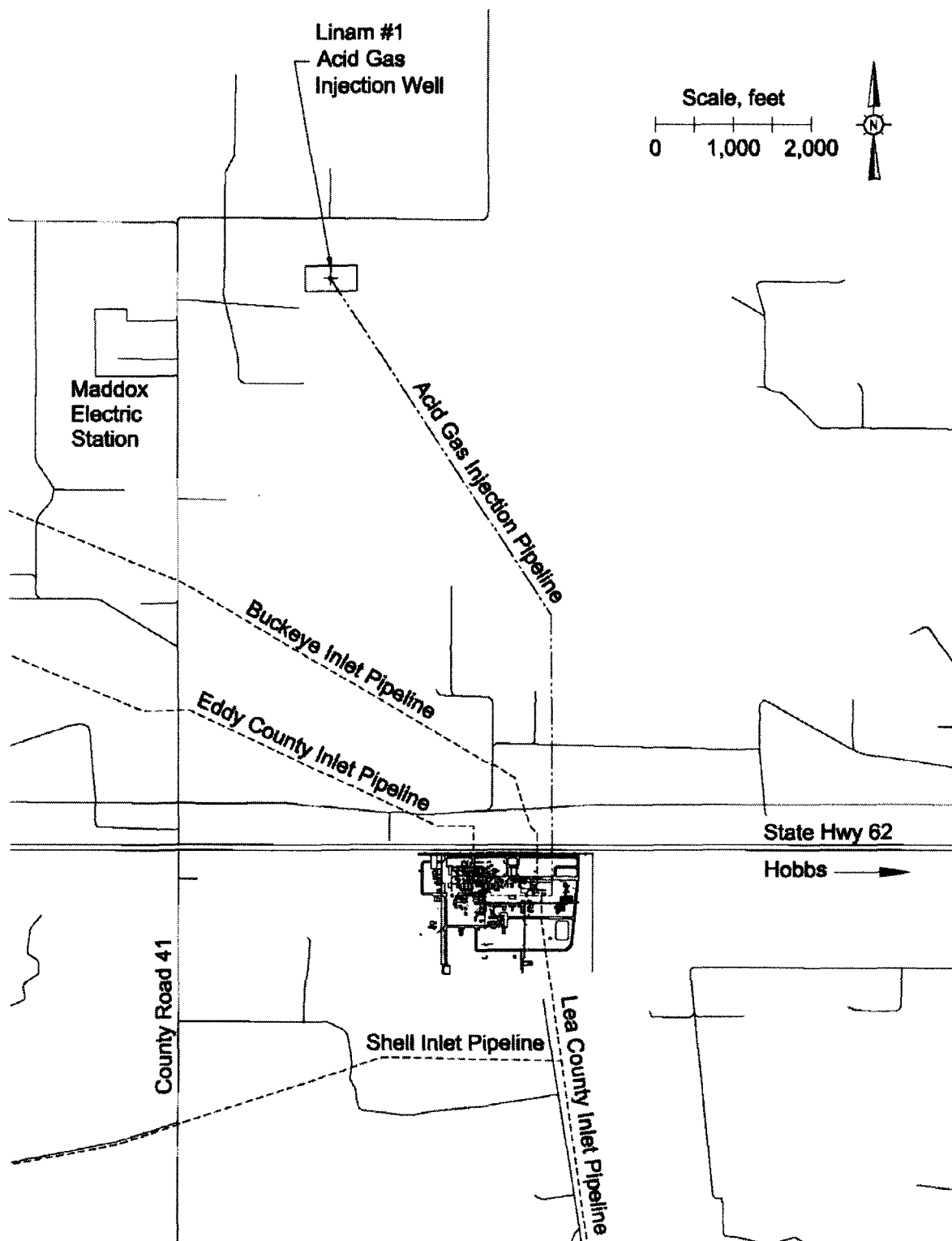
Figure 2-1
Regional Overview

2.3   Pipeline Data

A summary of pipeline data is presented in Table 2-1. The gas composition for each pipeline is presented in Table 2-2.

Table 2-1
Summary of Pipeline Data

Section	Pipe Diameter [inches]	Approximate Pressure at Plant Inlet [psia]	Temperature [°F]	Approximate Gas Flow Rate [mmscfd]
Buckeye	10	250	39	57
Eddy	12	250	46	95
Shell/Lea	12	250	53	48

Table 2-2
Representative Natural Gas Compositions

Component	Gas Composition [mol %]		
	Buckeye Pipeline	Eddy Pipeline	Shell/Lea Pipeline
Methane	73.15	81.29	87.18
Ethane	12.05	9.30	5.81
Propane	6.47	4.15	2.38
n-Butane	2.32	1.60	1.01
N-pentane	0.64	0.71	0.65
Hydrogen sulfide	0.84	0.39	0.17
Carbon dioxide	2.14	0.97	1.08
Nitrogen	2.38	1.60	1.72

2.4   Amine Unit

The natural gas streams from the three pipelines are combined at the plant. The resulting mixed stream is sent to an amine absorption unit to remove hydrogen sulfide and carbon dioxide. This system splits the incoming gas stream to feed four identical monoethanolamine (MEA) contactors. The gas streams leaving these contactors are recombined and sent on for further processing in the plant. The foul amine (amine containing H_2S) streams from the four contactors are combined in a flash tank and then split into two streams which are sent to two amine stills to regenerate the amine. The acid gas from the amine stills is then combined and sent on, either to the sulfur recover unit (SRU), or to be compressed and injected into a well using one of three reinjection options under consideration. A summary of equipment operating data for this unit is presented in Table 2-3.

QUEST

Table 2-3
Amine Unit Physical and Operating Data

Stream	Phase	Temperature [F]	Pressure [psia]	Mole Percent H₂S
Gas Inlet to Amine Unit	Gas	86	243	0.71
Amine Contactor Bottoms	Aqueous Liquid	115	243	0.60
Vapor From Amine Still	Gas	226	27	7.57
Acid Gas to SRU or Injection System	Gas	120	26.5	25.20

2.5   Sulfur Recovery Unit

The acid gas stream from the amine unit is currently processed in the SRU. In this unit, the acid gas is first mixed with air and burned in a reaction furnace to convert hydrogen sulfide into sulfur dioxide. With expansion to 200 mmscfd, the gas stream will be passed through a series of four converters to convert the remaining sulfur dioxide into elemental sulfur. After each converter, the stream passes through a condenser where liquid sulfur is removed before the gas stream and is passed to another reheater/converter/condenser stage. After the final condenser, the remaining gas stream is sent to an incinerator. A summary of equipment operating data for this unit is presented in Table 2-4.

Table 2-4
Sulfur Recovery Unit Physical and Operating Data

Stream	Temperature [F]	Pressure [psia]	Mole Percent SO₂	Mole Percent H₂S
Gas From Reaction Furnace	481	17.7	5.45	10.75
Inlet to Converter #2	386	16.7	1.04	1.80
Inlet to Converter #3	375	15.9	0.26	0.22
Inlet to Converter #4	339	15.4	0.10	0.15
SRU Tail Gas	258	15.4	0.10	0.38

2.6   Injection Options

2.6.1   Compression at Linam Ranch (Reinjection Option #1)

The first option under consideration for handling acid gas from the gas plant is to compress the acid gas to 2,250 psig at the Linam Ranch gas plant, transport the gas via a 3-inch buried pipeline to the acid gas injection (AGI) wellsite, and inject the gas into the reservoir.

QUEST

2.6.2 Split Compression (Reinjection Option #2)

A second option under consideration for handling acid gas from the gas plant is to compress the acid gas to 90 psig at the Linam Ranch gas plant, transport the gas via an 8-inch buried pipeline to the AGI wellsite, then compress the gas to 2,250 psig and inject the gas into the reservoir.

2.6.3 Compression at Injection Wellsite (Reinjection Option #3)

The final option under consideration for handling acid gas from the gas plant is to transport the acid gas via an 18-inch buried pipeline to the AGI wellsite, compress it to 2,250 psig at the wellsite, and inject the gas into the reservoir.

2.6.4 Compression Options Physical and Operating Data

A summary of the compression options for acid gas injection is given in Table 2-5.

Table 2-5
Summary of Physical and Operating Conditions for Compression Options

Option #	Outside Pipe Diameter [inches]	Fluid Phase	Pressure at Linam Ranch [psig]	Pressure at AGI Wellsite [psig]
1 – Compression at Linam Ranch	3"	Fluid	2,250	<2,250
2 – Split Compression	8"	Gas	90	2,250
3 – Compression at AGI wellsite	18"	Gas	4	2,250

2.7 Population Data

The gas plant and the majority of the Linam Ranch pipeline system are located in rural areas that are sparsely populated. None of the facilities associated with the current gas plant and the proposed reinjection pipeline have any residential or business structures within 2,000 feet. Because of these factors, the potential for the public to being exposed to an accidental release of gas is low.

2.8 Meteorological Data

Meteorological data for wind speed, wind direction, and Pasquill-Gifford atmospheric stability class used in this study were gathered from the Midland, Texas airport for the years 1995 through 2004. This was the nearest available reporting station with a complete data set and is approximately 70 nautical miles southeast of Hobbs, New Mexico. Figure 2-2 presents the annual wind rose data for all stability classes. The length and width of a particular arm of the rose define the frequency and speed at which the wind blows from the direction the arm is pointing. As an example, reviewing Figure 2-2 shows that the most common wind blows from south to north.
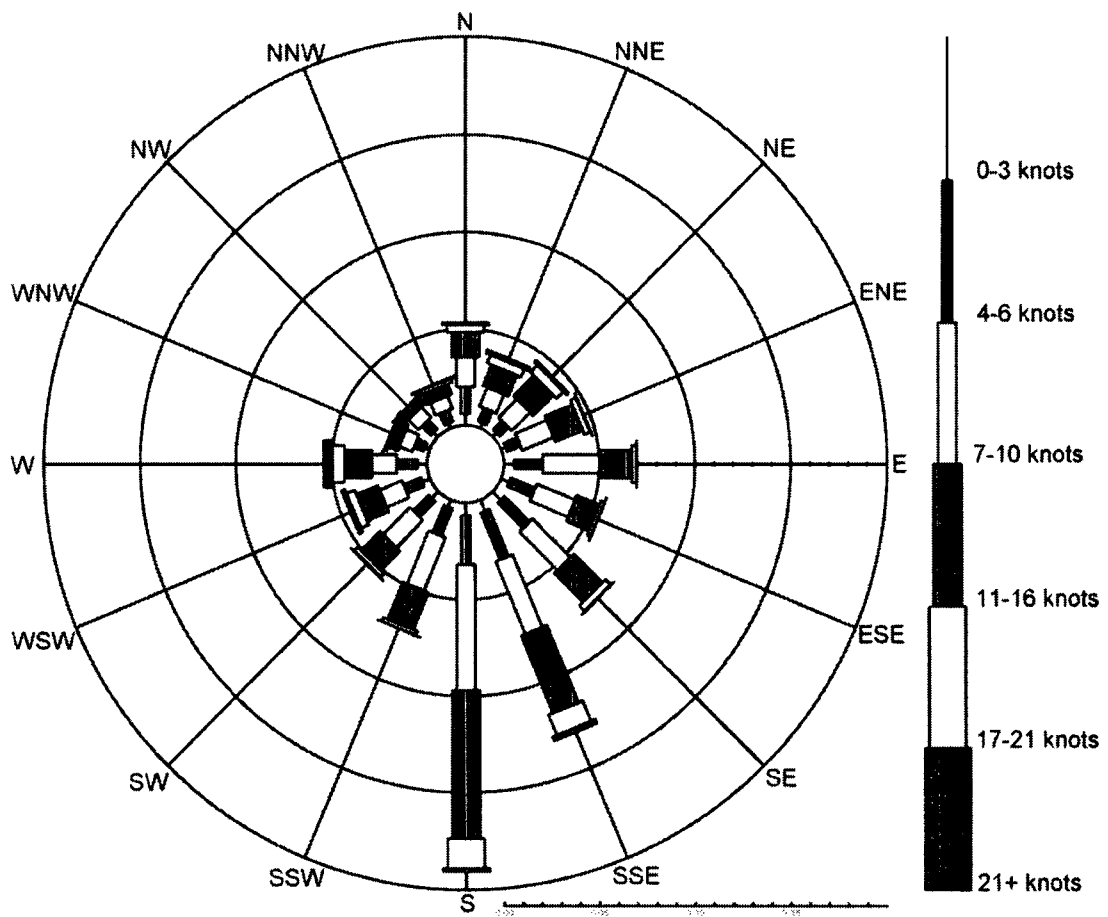
QUEST

Figure 2-2
Wind Rose for Midland, Texas

SECTION 3
POTENTIAL HAZARDS

Quest reviewed the Linam Ranch current and proposed pipeline routes, equipment locations, and reinjection options in order to determine credible hazardous release events involving H_2S and SO_2. As a result of this review, the following potential releases of toxic fluids were selected for evaluation.

Sour Gas Pipeline Releases

(1)   Full rupture of the pipeline or associated equipment, resulting in rapid depressurization of the line. This is considered the maximum credible release that might occur along a pipeline.

(2)   A 2-inch hole in one of the pipelines or associated equipment. This hole could be the result of material defect or puncture.

(3)   A 1/4-inch hole in one of the pipelines or associated equipment. This release would simulate a corrosion hole in the pipeline.

Amine Unit and Sulfur Recovery Unit

(1)   Full rupture of the piping or associated equipment, resulting in rapid depressurization of the system.

(2)   A 1-inch hole in the piping or associated equipment. This hole could be the result of material defect or puncture.

(3)   A 1/4-inch hole in the piping or associated equipment. This release would simulate a corrosion hole or a damaged fitting in the equipment.

Injection Compression Equipment

(1)   Full rupture of the piping or associated equipment, resulting in rapid depressurization of the system.

(2)   A 1-inch hole in the compression equipment. This hole could be the result of material defect or puncture.

(3)   A 1/4-inch hole in the compression or associated equipment. This release would simulate a corrosion hole or a damaged fitting in the equipment.

Wellhead Releases

(1)   A well blowout created by a full rupture or massive failure of the wellhead, with subsequent failure of the subsurface safety valve (SSSV) and the check valve located at the bottom of the well. This release could continue for hours or even days.

(2)   A full rupture or massive failure of the wellhead in which the SSSV closes promptly. In this scenario, the release is fed by the pipeline system, not by the reservoir.

(3)   A 1-inch hole in wellhead equipment. This hole might be the result of a material defect or puncture. The release is treated as an aboveground pipeline release.

(4)   A 1/4-inch hole in wellhead equipment. This hole simulates a fitting failure or a corrosion hole in the equipment. The release is treated as an aboveground pipeline release.

Hazards Created by Releases

The release scenarios described above define the range of credible releases that might occur along the pipeline routes or in the processing units. Each of these releases may create one or more of the following toxic hazards.

QUEST

(1)   Exposure to gas containing H_2S.

(2)   Exposure to gas containing SO_2.

The remainder of Section 3 defines the techniques used to quantify the hazards, while Section 4 quantifies the frequencies at which these releases might occur.

3.1   Physiological Effects of Hydrogen Sulfide

H_2S is a colorless, toxic, flammable gas with a strong, irritating odor. H_2S has a low threshold limit value (TLV) and is detectable by odor at concentrations significantly lower than those necessary to cause physical harm or impairment (odor detectable from 0.13 – 1 ppm). The most serious hazard presented by H_2S is exposure to a large release from which escape is impossible. Table 3-1 describes various physiological effects of H_2S.

The physiological effects of airborne toxic materials depend on the concentration of the toxic vapor in the air being inhaled, and the length of time an individual is exposed to this concentration. The combination of concentration and time is referred to as "dosage." In risk studies that involve toxic gases, probit equations are commonly used to quantify the expected rate of fatalities for the exposed population. Probit equations are based on experimental dose-response data and take the following form.

$$P_r = a + b \ln (C^n \times t)$$

where: P_r probit
                     C concentration of toxic vapor in the air being inhaled (ppm)
                     t time of exposure (minutes) to concentration C
                     a, b, and n constants

The product $C^n \times t$ is often referred to as the "dose factor." According to probit equations, all combinations of concentration (C) and time (t) that result in equal dose factors also result in equal values for the probit (P_r) and therefore produce equal expected fatality rates for the exposed population.

3.1.1 H_2S Probit Relation from the Center for Chemical Process Safety

A probit equation for H_2S has been presented by the Center for Chemical Process Safety [CCPS, 1989]. This probit uses the values of -31.42, 3.008, and 1.43 for the constants a, b, and n, respectively. Substituting these values into the general probit equation yields the following probit equation for H_2S.

$$P_r = -31.42 + 3.008 \ln (C^{1.43} \times t)$$

Dispersion calculations are often performed assuming a 60-minute exposure to the gas. This is particularly true when dealing with air pollution studies since they are typically concerned with long-term exposures to low concentration levels. For accidental releases of toxic gases, shorter exposure times are warranted since the durations of many accidental releases are often less than an hour. In this study, calculations were performed for various exposure times and concentration levels, dependent on the duration and nature of the release.

Table 3-1

Physiological Response to Various Concentrations of Hydrogen Sulfide (H2S)

H2S Concentration [ppm]	Duration of Exposure						
	0-2 min	2-15 min	15-30 min	30 min to 1 hr	1-4 hr	4-8 hr	8-48 hr
5-100				Mild conjunctivitis, respiratory tract irritation.			
100-150		Coughing, irritation of eyes, loss of sense of smell.	Disturbed respiration, pain in eyes, sleepiness.	Throat irritation.	Salivation and mucous discharge, sharp pain in eyes, coughing.	Increased symptoms.*	Hemorrhage and death.*
150-200		Loss of sense of smell.	Throat and eye irritation.	Throat and eye irritation.	Difficult breathing, blurred vision, light shy.	Serious irritating effect.*	Hemorrhage and death.*
250-350	Irritation of eyes, loss of sense of smell.	Irritation of eyes.	Painful secretion of tears, weariness.	Light shy, nasal catarrh, pain in eyes, difficult breathing.	Hemorrhage and death.*		
340-450		Irritation of eyes, loss of sense of smell.	Difficult respiration, coughing, irritation of eyes.	Increased irritation of eyes and nasal tract, dull pain in head, weariness, light shy.	Dizziness, weakness, increased irritation, death.	Death.*	
500-600	Coughing, collapse, and unconsciousness.	Respiratory disturbances, irritation of eyes, collapse.*	Serious eye irritation, light shy, palpitation of heart, a few cases of death.	Severe pain in eyes and head, dizziness, trembling of extremities, great weakness and death.*			
600 or greater	Collapse, unconsciousness, death.*						

*Data secured from experience on dogs that have a susceptibility similar to man.
Source: National Safety Council data sheet D-chem 15.

3-3

QUEST

When using a probit equation, the value of the probit (P_r) that corresponds to a specific dose factor must be compared to a statistical table to determine the expected mortality (fatality) rate. If the value of the probit is 2.67, the expected mortality rate is 1%. Using the CCPS probit equation given above, the dose factor that equates to a one percent mortality rate is 256 ppm for 30 minutes, or 157 ppm for a 60-minute exposure, or 416 ppm for a 15-minute exposure, etc., as shown in Table 3-2. Table 3-2 presents the probit values, mortality rates, and H_2S concentrations for various exposure times, while Figure 3-1 presents the same information in graphical form.
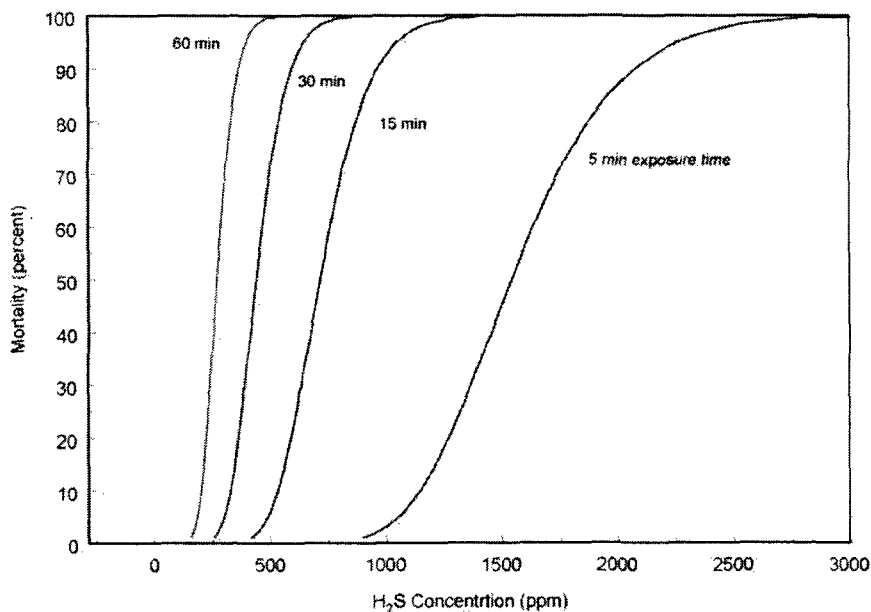
Figure 3-1
Toxic Probit Relationships for Hydrogen Sulfide (H_2S)

Table 3-2
Hazardous H₂S Concentration Levels for Various Exposure Times
Using the CCPS H₂S Probit

Exposure Time [minutes]	Probit Value	Mortality Rate* [percent]	H₂S Concentration [ppm]
5	2.67	1	897
	5.00	50	1,542
	7.33	99	2,648
15	2.67	1	416
	5.00	50	715
	7.33	99	963
30	2.67	1	256
	5.00	50	440
	7.33	99	756
60	2.67	1	157
	5.00	50	271
	7.33	99	465

*Percent of exposed population fatally affected.

3.2   Physiological Effects of Sulfur Dioxide

SO₂ is a colorless, nonflammable, toxic gas with a strong, irritating odor. SO₂ is so irritating that it provides its own warning of toxic concentration (odor detectable from 0.3 – 1 ppm). Similar to H₂S, the most serious hazard presented by SO₂ is exposure to a large release from which escape is impossible. The principle toxic effects of SO₂ are due to the formation of sulfurous acid when SO₂ comes into contact with water in bodily fluids.

3.2.1   SO₂ Probit Relation from the Center for Chemical Process Safety

A probit equation for SO₂ has been presented by the Center for Chemical Process Safety [CCPS, 1989]. This probit uses the values of -15.67, 2.100, and 1.00 for the constants a, b, and n, respectively. Substituting these values into the general probit equation yields the following probit equation for SO₂.

$$P_r = 15.67 \quad 2.100 \ln (C^{1.00} \times t)$$

Using the CCPS probit equation given above, the dose factor that equates to a one percent mortality rate is 103 ppm for 60 minutes exposure, or 207 ppm for 30 minutes exposure, or 414 ppm for 15 minutes exposure, etc., as shown in Table 3-3. Table 3-3 presents the probit values, mortality rates, and SO₂ concentrations for various exposure times, while Figure 3-2 presents the same information in graphical form.

QUEST

Table 3-3
Hazardous SO$_2$ Concentration Levels for Various Exposure Times
Using the CCPS SO$_2$ Probit

Exposure Time [minutes]	Probit Value	Mortality Rate* [percent]	SO$_2$ Concentration [ppm]
5	2.67	1	1,241
	5.00	50	3,765
	7.33	99	11,418
15	2.67	1	414
	5.00	50	1,255
	7.33	99	3,806
30	2.67	1	207
	5.00	50	628
	7.33	99	1,903
60	2.67	1	103
	5.00	50	314
	7.33	99	952

*Percent of exposed population fatally affected.
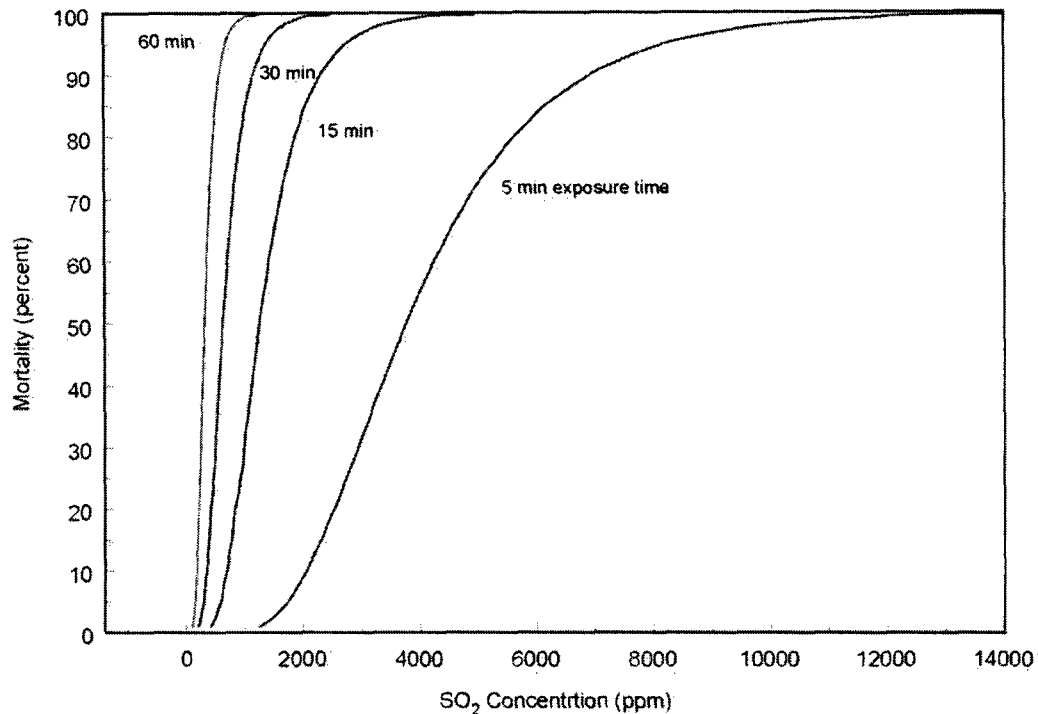
Figure 3-2
Toxic Probit Relationships for Sulfur Dioxide (SO$_2$)

QUEST

3-6

3.3 Consequence Analysis

When performing site-specific consequence analysis studies, the ability to accurately model the release, dilution, and dispersion of gases and aerosols is important if an accurate assessment of potential exposure is to be attained. For this reason, Quest uses a modeling package, CANARY by Quest®, that contains a set of complex models that calculate release conditions, initial dilution of the vapor (dependent upon the release characteristics), and the subsequent dispersion of the vapor introduced into the atmosphere. The models contain algorithms that account for thermodynamics, mixture behavior, transient release rates, gas cloud density relative to air, initial velocity of the released gas, and heat transfer effects from the surrounding atmosphere and the substrate. The release and dispersion models contained in the QuestFOCUS package (the predecessor to CANARY by Quest) were reviewed in a United States Environmental Protection Agency (EPA) sponsored study [TRC, 1991] and an American Petroleum Institute (API) study [Hanna, Strimaitis, and Chang, 1991]. In both studies, the QuestFOCUS software was evaluated on technical merit (appropriateness of models for specific applications) and on model predictions for specific releases. One conclusion drawn by both studies was that the dispersion software tended to overpredict the extent of the gas cloud travel, thus resulting in too large a cloud when compared to the test data (i.e., a conservative approach).

A study prepared for the Minerals Management Service [Chang, et al.,1998] reviewed models for use in modeling routine and accidental releases of flammable and toxic gases. CANARY by Quest received the highest possible ranking in the science and credibility areas. In addition, the report recommends CANARY by Quest for use when evaluating toxic and flammable gas releases. The specific models (e.g., SLAB) contained in the CANARY by Quest software package have also been extensively reviewed.

Technical descriptions of the CANARY models used in this study are presented in Appendix A.

3.3.1 Source Term Initialization for Aqueous Amine Releases

The evolution rate of hydrogen sulfide from the surface of a pool of foul monoethanolamine (MEA) presents a modeling problem that cannot be handled using the models present in CANARY by Quest. To correctly calculate this rate so that the dispersion of hydrogen sulfide from these pools can be determined, the equation presented by Stiver and Mackay [1983] is used:

$$\frac{N}{A} = \frac{P_p \, k \, MW}{R \, T}$$

where:

$\dfrac{N}{A}$ mass vaporization rate of contaminant per unit area of pool surface, kg/m^2.

P_p partial pressure of contaminant over surface of pool, kPa

MW molecular weight of contaminant, kg/kg-mol

R universal gas law constant, $kPa*m^3/kg\text{-}mol*K$

T temperature of pool surface, K

k mass transfer coefficient, m/s

k is given by Stiver and Mackay as:

$$k = 0.002 \, u$$

where: u = wind speed at the surface of the pool, m/s

It was assumed that the rate-limiting step in the volatilization of hydrogen sulfide from the solution was the mass transfer step. It was also assumed that there was sufficient hydrogen sulfide in solution and that its concentration was sufficient to maintain this partial pressure for the duration of the releases. Both of these

QUEST

assumptions are conservative in that if they are not met, the actual rate of evolution of hydrogen sulfide from the pool will be lower and the consequent dispersion distances will be smaller.

3.3.2 Toxic Concentration Limits for the SRU Releases

Both H_2S and SO_2 are present in gas streams within the SRU. In the absence of data on the combined effect of these toxic gases on humans, the toxic hazards of each gas must be determined individually. To determine which component in each of the gas streams presents the largest impact zone, a representative accident was analyzed. The gas stream from the SRU reaction furnace was chosen as it contains the largest concentration of both toxic gases in the SRU. The composition of this stream is given in Table 3-4.

Table 3-4
SRU Reaction Furnace Gas Stream Composition

Component	Mole Fraction
Nitrogen	0.346975
Carbon Dioxide	0.391878
Hydrogen Sulfide	0.107541
Sulfur Dioxide	0.054514
Water	0.099092

The toxic endpoints chosen for this analysis were the 60 minute 1%, 50%, and 99% fatality probit concentration levels for H_2S and SO_2.

In order to determine wether H_2S or SO_2 produces the largest impact, vapor dispersion calculations were performed that tracked the dispersion of each. Figures 3-3 and 3-4 show the results of these calculations.

QUEST

CONCENTRATION CONTOURS: OVERHEAD VIEW
Momentum Jet Cloud
Gas from reaction furnace - H2S
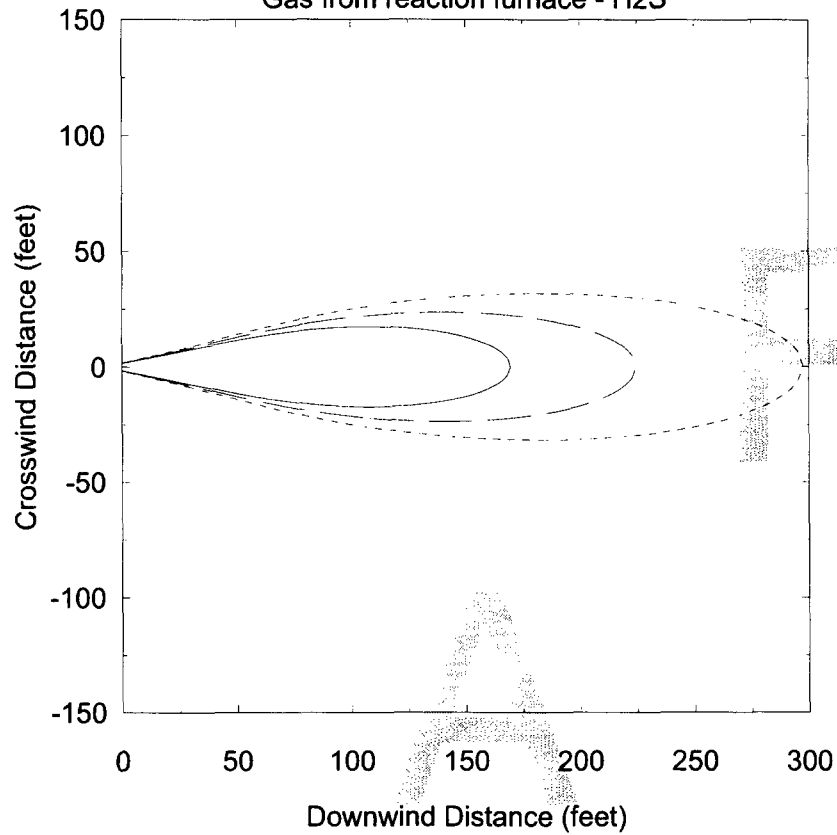
————— 465 ppm Hydrogen Sulfide   casename=31vfxr_a
— —   271 ppm Hydrogen Sulfide   windspeed = 4.5 mph
- - - - 157 ppm Hydrogen Sulfide   D stability
CANARY by Quest   Thu Sep 22 10:21:57 2005

Figure 3-3
Hydrogen Sulfide Dispersion Following Release from SRU Reaction Furnace

QUEST

CONCENTRATION CONTOURS: OVERHEAD VIEW
Momentum Jet Cloud
Gas from reaction furnace - SO2

——	952 ppm Sulfur Dioxide	casename=31vfxr_b
— —	314 ppm Sulfur Dioxide	windspeed = 4.5 mph
- - - -	103 ppm Sulfur Dioxide	D stability
CANARY by Quest		Thu Sep 22 10:22:26 2005
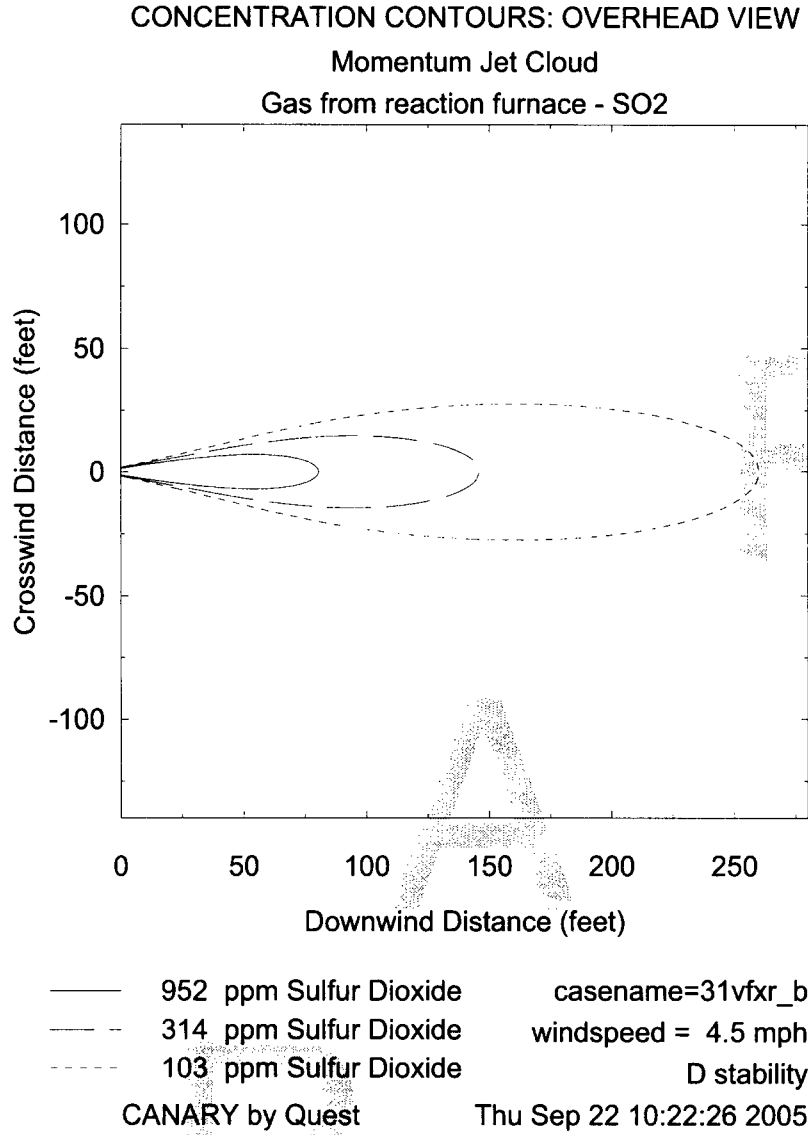
Figure 3-4
Sulfur Dioxide Dispersion Following Release from SRU Reaction Furnace

QUEST

A comparison of the two figures illustrates that hydrogen sulfide generates a larger impact zone for all three probit levels of concern. For this reason, hydrogen sulfide was the toxic component chosen to determine the hazard distances from the SRU.

3.3.3 Dispersion Analysis Results – Acid Gas Stream Releases From the Amine Unit

Table 3-5 contains the maximum downwind travel distances to the three H_2S concentrations of interest (897 ppm, 1,542 ppm, and 2,652 ppm for five-minute exposures) evaluated for the full rupture scenario on the acid gas stream exiting from the amine unit. Results for each of the twenty-one wind speed/atmospheric stability conditions that occur at the Linam Ranch site are presented in the matrix .

Similar information is generated for 1-inch puncture and 1/4-inch corrosion hole releases and are presented in Tables 3-6 and 3-7 , respectively. In the analysis, the rupture, puncture, and 1/4-inch releases were calculated for all inlet pipelines, gas processing equipment, compression equipment, and the injection well options.

QUEST

Maximum downwind distances
Full rupture - Acid gas line from amine unit

C low	(mole fraction)	897 ppm H_2S	(1% mortality)
C middle	(mole fraction)	1,542 ppm H_2S	(50% mortality)
C high	(mole fraction)	2,652 ppm H_2S	(99% mortality)

Downwind Distance in Feet to Concentration Level

	A stability	B stability	C stability	D stability	E stability	F stability
11.32 m/s wind speed			335 255 193	371 281 211		
10.36 m/s wind speed			359 274 207	395 300 225		
7.20 m/s wind speed			458 353 267	498 378 283		
4.63 m/s wind speed		428 345 275	527 419 327	593 464 356	659 507 382	
2.83 m/s wind speed	388 319 261	471 386 313	569 462 372	651 625 419	705 565 449	835 655 507
1.03 m/s wind speed	434 361 300	506 423 352	606 507 424	681 571 477		962 806 673

Note: wind speed/stability combinations which normally occur are enclosed by the heavy line.

QUEST

Table 3-6
Toxic Gas Dispersion Results – 1-Inch Hole in Acid Gas Line from Amine Unit

Maximum downwind distances
1-inch hole in Acid gas line from amine unit

C low	(mole fraction)	509 ppm H$_2$S	(1% mortality)
C middle	(mole fraction)	875 ppm H$_2$S	(50% mortality)
C high	(mole fraction)	1,505 ppm H$_2$S	(99% mortality)

Downwind Distance in Feet to Concentration Level

	A stability	B stability	C stability	D stability	E stability	F stability
11.32 m/s wind speed			102 77 57	111 83 62		
10.36 m/s wind speed			110 83 61	120 90 67		
7.20 m/s wind speed			146 110 81	158 118 87		
4.63 m/s wind speed		166 124 91	200 149 109	213 158 116	225 167 121	
2.83 m/s wind speed	187 138 99	227 167 121	261 192 138	272 199 143	283 206 147	301 211 147
1.03 m/s wind speed	271 209 150	323 244 177	367 274 198	388 287 208		459 340 245

Note: wind speed/stability combinations which normally occur are enclosed by the heavy line.

QUEST

Table 3-7
Toxic Gas Dispersion Results – 1/4-Inch Hole in Acid Gas Line from Amine Unit

Maximum downwind distances
1/4-inch hole in Acid gas line from amine unit

C low	(mole fraction)	157 ppm H_2S	(1% mortality)
C middle	(mole fraction)	271 ppm H_2S	(50% mortality)
C high	(mole fraction)	466 ppm H_2S	(99% mortality)

Downwind Distance in Feet to Concentration Level

	A stability	B stability	C stability	D stability	E stability	F stability
11.32 m/s wind speed			41 / 31 / 23	45 / 34 / 25		
10.36 m/s wind speed			44 / 33 / 24	49 / 37 / 28		
7.20 m/s wind speed			61 / 46 / 34	66 / 50 / 38		
4.63 m/s wind speed		70 / 53 / 39	87 / 66 / 49	93 / 71 / 53	100 / 76 / 57	
2.83 m/s wind speed	79 / 59 / 42	102 / 76 / 56	124 / 94 / 70	132 / 100 / 74	139 / 105 / 78	152 / 114 / 84
1.03 m/s wind speed	130 / 95 / 67	164 / 121 / 88	190 / 143 / 105	200 / 150 / 110		245 / 184 / 136

Note: wind speed/stability combinations which normally occur are enclosed by the heavy line.

QUEST

3.4   Summary of Consequence Analysis Results

Table 3-8 presents a summary of the largest impacts from each of the Linam Ranch gas plant sections and options evaluated in this study. In each table, the maximum ground level distances to the specified hazard endpoints are listed for ruptures, punctures, and leaks from project equipment.

QUEST

Table 3-8
Largest Toxic Hazard Distances for H$_2$S Releases
from Linam Ranch Gas Plant and Reinjection Systems

Release from	Distance [ft] from Release Point to Fatality Level		
	1%	50%	99%
Buckeye Inlet Pipeline	30	7	5
Eddy Inlet Pipeline	12	8	6
Shell/Lea Inlet Pipeline	5	3	2
Combined Gas Inlet to Plant	80	*	*
Inlet Receivers	100	*	*
Gas Inlet to Individual Amine Contactor	125	65	16
Contactor Rich Amine Outlet	70	52	39
Flash Drum Rich Amine Outlet	70	52	39
Amine Still Rich Amine Inlet	120	90	70
Vapor Line from Amine Still	42	*	*
Acid Gas to SRU or Injection Pipeline	960	810	675
Reaction Furnace Outlet	465	370	260
Inlet Line to Converter #2	170	110	65
Inlet Line to Converter #3	19	*	*
Inlet Line to Converter #4	10	*	*
SRU Tail Gas Line	25	16	*
Sulfur Condenser	3	3	3
Sulfur Pit	3	3	3
Acid Gas Compressor at Gas Plant (Option #1)	1,380	1,125	910
3" Acid Gas Pipeline (Option #1)	1,435	1,165	935
Above-ground 3" Acid Gas Line at AGI Wellsite (Option #1)	1,520	1,290	1,090
First Stage Acid Gas Compressor (Option #2)	670	550	450
8" Acid Gas Pipeline (Option #2)	675	480	*
Aboveground 8" Acid Gas Line (Option #2)	1,055	855	685
Second Stage Acid Gas Compressor (Option #2)	1,400	1,145	920
Aboveground (in-plant) 18" Acid Gas Line (Option #3)	940	790	655
18" Acid Gas Pipeline (Option #3)	1,150	940	760
Acid Gas Compressor at AGI wellsite (Option #3)	1,410	1,150	930
Wellhead Tubing with SSSV Failure and Down-hole Check Valve Closure †	1,815	1,550	1,315
Wellhead Tubing with SSSV Failure and Down-hole Check Valve Failure ‡	4,185	3,300	2,595

* Endpoint not reached at grade
† Double-failure scenario
‡ Triple-failure scenario

QUEST

SECTION 4
ACCIDENT FREQUENCY

The likelihood of a particular accident occurring within some specific time period can be expressed in different ways. One way is to state the statistical probability that the accident will occur during a one-year period. This annual probability of occurrence can be derived from failure frequency data bases of similar accidents that have occurred with similar systems or components in the past.

Most data bases (e.g., CCPS [1989], OREDA [1984]) that are used in this type of analysis contain failure frequency data (e.g., on the average, there has been one failure of this type of equipment for 347,000 hours of service). By using the following equation, the annual probability of occurrence of an event can be calculated if the frequency of occurrence of the event is known.

$$p = 1 - e^{(-\lambda t)}$$

where:
  p annual probability of occurrence (dimensionless)
  λ annual failure frequency (failures per year)
  t time period (one year)

If an event has occurred once in 347,000 hours of use, its annual failure frequency is computed as follows.

$$\lambda = \frac{1\ event}{347,000\ hours} \times \frac{8,760\ hours}{year} = 0.0252\ events/year$$

The annual probability of occurrence of the event is then calculated as follows.

$$p = 1 - e^{(-0.0252 \cdot 1)} = 0.0249$$

Note that the frequency of occurrence and the probability of occurrence are nearly identical. (This is always true when the frequency is low.) An annual probability of occurrence of 0.0249 is approximately the same as saying there will probably be one event per forty years of use.

Due to the scarcity of accident frequency data bases, it is not always possible to derive an exact probability of occurrence for a particular accident. Also, variations from one system to another (e.g., differences in design, operation, maintenance, or mitigation measures) can alter the probability of occurrence for a specific system. Therefore, variations in accident probabilities are usually not significant unless the variation approaches one order of magnitude (i.e., the two values differ by a factor of ten).

The following subsections describe the basis and origin of failure frequency rates used in this analysis.

4.1   Piping Failure Rates

4.1.1   Welded Piping

WASH-1400 [USNRC, 1975] lists the failure rates for piping as 1.0×10^{-10}/hour for pipes greater than three inches in diameter, and 1.0×10^{-9}/hour for smaller pipes. These rates are based on a "section" of pipe, i.e., 1.0×10^{-10} failures per section of >three-inch pipe/hour. A section of pipe is defined as any straight portion

QUEST

of pipe of welded construction between any two fittings (such as flanges, valves, strainers, elbows, etc.). CCPS [1989] gives a mean pipe failure rate of 2.68×10^{-8}/mile/hour (4.45×10^{-8}/foot/year). This would be approximately the same as the WASH-1400 rate, 1.0×10^{-9}/section/hour (8.76×10^{-6}/section/year), if the average section of pipe were about 200 feet in length.

Most data bases of pipe failure rates are not sufficiently detailed to allow a determination of the failure frequency as a function of the size of the release (i.e., size of the hole in the pipe). However, British Gas has gathered such data on their gas pipelines [Fearnehough, 1985]. Their data show that well over 90% of all failures are less than a one-inch diameter hole, and only 3% are greater than a three-inch diameter hole. Since most full ruptures of piping systems are caused by outside forces, full ruptures are expected to occur more frequently on small-diameter pipes.

Based on the above discussion, the expected failure rates for aboveground, metallic piping with no threaded connections are assumed to be as follows.

For pipes from one inch to three inches in diameter:

Hole size	1/4 inch	1/4 to 1 inch	1 inch to full rupture
Expected failure rate	2.25×10^{-8}/foot/year	1.8×10^{-8}/foot/year	4.5×10^{-9}/foot/year

For pipes from four inches to ten inches in diameter:

Hole size	1/4 inch	1/4 to 1 inch	1 inch to full rupture
Expected failure rate	2.25×10^{-8}/foot/year	2.0×10^{-8}/foot/year	2.5×10^{-9}/foot/year

4.1.2   Screwed Piping

CCPS [1989] also gives a value of 5.7×10^{-7}/hour for the failure rate of metal piping connections. The specific types of connections are not listed, but threaded connections are implied since failures in welded piping systems with flanged connections are either classified as piping failures or gasket failures. Failure rates for piping in aboveground, metallic piping systems with screwed connections are assumed to be the same as the failure rates listed in Section 4.1.1 for welded piping systems. For screwed fittings, the expected failure rates are as follows.

Hole size	0 to 1/4 inch	1/4 inch to full rupture
Expected failure rate	4.0×10^{-3}/fitting/year	1.0×10^{-3}/fitting/year

4.2   Gaskets

According to WASH-1400 [USNRC, 1975], the median failure rate (leak or rupture) for gaskets at flanged connections is 3.0×10^{-7}/hour. Green and Bourne [1972] reported 5.0×10^{-7}/hour as the failure rate for gaskets. The data from both sources are thought to include small leaks that would not create significant hazards.

Unfortunately, the data are not broken down by gasket type. It is generally believed that spiral-wound, metallic-reinforced gaskets are less prone to major leaks than ordinary composition gaskets. Also, it is nearly impossible to "blow out" all, or even a section, of a metallic-reinforced gasket. In consideration of these factors, a failure rate of 3.0×10^{-8}/hour is thought to be conservative for loss of 1/4 of a metallic-reinforced gasket. Based on continuous service, the annual expected failure rate for metallic-reinforced gaskets is 2.6

QUEST

x 10^{-4} failures/year/gasket. For ordinary composition gaskets, the expected failure rate is 2.6 x 10^{-3} failures/year/gasket.

4.3 Valves

4.3.1 Valve Leaks and Ruptures

WASH-1400 [USNRC, 1975] lists a failure rate of 1.0 x 10^{-8} failures/hour for external leakage or rupture of valves. Assuming continuous service, the annual leakage/rupture rate is approximately 8.8 x 10^{-5}/year. Unfortunately, this number includes very small leaks as well as valve body ruptures. This reduces the usefulness of this failure rate since the probability of a small leak from a valve bonnet gasket is obviously much greater than the probability of a one-inch hole in the valve body. To overcome this difficulty, the valve body can be considered similar to pipe, and the valve bonnet gasket can be treated like other gaskets. To be conservative, each flanged valve is considered to have a failure rate equal to a ten-foot section of pipe and one gasket. Similarly, a threaded valve is treated like ten feet of pipe, one gasket, and one screwed fitting.

4.3.2 Check Valve failures

The CCPS [1989] lists a value for the failure of a check valve to prevent reverse flow upon demand. This value is 2.2 failures per 1,000 demands, or 2.2 x 10^{-3}/d.

4.4 Pressure Vessel Failure Rates

4.4.1 Leaks

CCPS [1989] reports a failure rate of 1.09 x 10^{-8}/hour for pressure vessels. For continuous service, the annual expected failure rate for pressure vessels would be 9.5 x 10^{-5} failures/year. Bush [1975] made an in-depth study of pressure vessels of many types, including boilers. In Bush's study, the rate of "disruptive" failures of pressure vessels was 1.0 x 10^{-5}/year, i.e., a factor of ten less than the CCPS value. The explanation for this difference lies in the definition of "failure." Bush's number is based on "disruptive" failures which are assumed to be failures of such magnitude that the affected vessel would need to be taken out of service immediately for repair or replacement. The data base reported by the CCPS most likely includes smaller leaks that Bush categorized as "noncritical."

Smith and Warwick [1981] analyzed the failure history of a large number of pressure vessels (about 20,000) in the United Kingdom. They present a short description of each failure, thus allowing the failures to be categorized by size. Most of the failures were small leaks (approximately half can be categorized as smaller than a one-inch diameter hole).

Based on the previous discussion, the following failure rates are proposed for pressurized process vessels.

Equivalent hole diameter	1/4 inch	1/4 to 1 inch	>1 inch
Expected failure rate	3.0 x 10^{-5}/year	4.0 x 10^{-5}/year	5.0 x 10^{-6}/year

QUEST

4.4.2 Catastrophic Failures

For this study, a catastrophic failure is defined as the sudden, nearly instantaneous rupture of a pressure vessel, resulting in nearly instantaneous release of the vessel's contents. Catastrophic failures of pressure vessels can be roughly divided into two types—cold catastrophic failures and BLEVE's.

If a pressure vessel ruptures when the contents of the vessel are at, or near, ambient temperature, the failure is a cold catastrophic failure. Such failures might occur as the result of improper metallurgy, defective welds, overpressurization, etc. Most products that are stored at ambient temperature in pressure vessel storage tanks are superheated liquefied gases. If the contents of the tank are released into the atmosphere nearly instantaneously, an aerosol cloud will be formed as some of the liquid flashes to vapor. If the material is flammable, the cloud might be ignited (either instantaneously or after some delay) or will dissipate without being ignited.

Sooby and Tolchard [1993] conducted an analysis of cold catastrophic failures of pressurized LPG storage tanks in Europe. They found that no such failure had ever been recorded during more than twenty-five million tank-years of service. From this data, they derived a frequency of 2.7×10^{-8} cold catastrophic failures per vessel per year for pressurized storage tanks.

The other type of catastrophic failure that is of interest is a BLEVE (Boiling Liquid Expanding Vapor Explosion). A typical BLEVE scenario involves a fire external to the pressure vessel. The contents of the tank are heated well above ambient temperature by the heat of the fire before the tank ruptures. Much of the liquid flashes upon release to the atmosphere and the external fire ignites the resultant aerosol cloud, thus creating a fireball of short duration.

An extensive risk analysis conducted by the United Kingdom Health and Safety Executive [HSE, 1991] estimated the frequency of BLEVE's for stationary LPG storage tanks is 1.8×10^{-7} per tank per year.

4.5   Heat Exchanger Failure Rates

Failure rate data for shell-and-tube heat exchangers that are designed and constructed much like other pressurized process vessels are sometimes reported with the data for pressure vessels. However, shell-and-tube heat exchangers are expected to have higher failure rates than simple pressure vessels because they are more complex than pressure vessels and are subject to additional stresses caused by temperature-induced expansion and contraction. To account for the additional complexity and stresses, the failure rates of the reboilers are assumed to be twice the rates listed previously for pressure vessels.

Based on this discussion, the following failure rates are proposed.

Equivalent hole diameter	1/4 inch	1/4 to 1 inch	>1 inch
Expected failure rate	6.0×10^{-5}/year	8.0×10^{-5}/year	1.0×10^{-5}/year

4.6   Compressor Failure Rates

Data on the frequency of releases from compressors are very rare, and contain little detailed information. A report from The Oil Industry International Exploration and Production Forum (E&P Forum) includes data from four sources, but the total sample size of all four data bases is only 1,875 compressor years of service [E&P, 1992]. The number of reported releases was 119, which translates to a release frequency of 6.35×10^{-2}/compressor/year. Only seven of the 119 releases were classified as "major."

QUEST

Based on this limited data, the expected failure rates are as follows.

Hole size	<1/4 inch	1/4 to 1 inch	1 inch to full rupture
Expected failure rate	6.0×10^{-2}/compr/yr	3.2×10^{-3}/compr/yr	5.3×10^{-4}/compr/yr

4.7   Pipeline Failure Rates

4.7.1   Steel Pipelines

Department of Transportation (DOT) data for underground liquid pipelines in the United States indicate a failure rate of 1.35×10^{-3} failures/mile/year [DOT 1988]. Data compiled from DOT statistics on failures of gas pipelines show a failure rate of 1.21×10^{-3} failures/mile/year for steel pipelines in the United States [Jones, et al., 1986]. In addition to failures of buried pipe, these data include failures of buried pipeline components, such as block valves and check valves, when the failure resulted in a release of fluid from the pipeline.

Data gathered by operators of gas transmission pipelines in Europe indicate a failure rate of 1.13×10^{-3} failures/mile/year [EGPIDG, 1988].

These data sets are not sufficiently detailed to allow a determination of the failure frequency as a function of the size of the release (i.e., the size of hole in the pipeline). However, British Gas has gathered such data on their gas pipelines [Fearnehough, 1985]. These data indicate that well over 90% of all failures are less than a one-inch diameter hole, and only 3% are greater than a three-inch diameter hole.

Data compiled from DOT data on gas pipelines in the United States show a trend toward higher failure rates as pipe diameter decreases [Jones, et al., 1986]. (Smaller diameter pipes have thinner walls; thus, they are more prone to failure by corrosion and by mechanical damage from outside forces.)

Based on the data sets described above, the expected failure rates for steel pipelines are assumed to be as follows.

For pipelines from six to twelve inches in diameter:

Hole size	<1/4 inch	1/4 to 1 inch	1 inch to full rupture
Expected failure rate	0.76×10^{-3}/mile/year	0.61×10^{-3}/mile/year	0.15×10^{-3}/mile/year

For pipelines from fourteen to twenty-two inches in diameter:

Hole size	<1/4 inch	1/4 to 1 inch	1 inch to full rupture
Expected failure rate	0.65×10^{-3}/mile/year	0.52×10^{-3}/mile/year	0.13×10^{-3}/mile/year

For pipelines from twenty-four to twenty-eight inches in diameter:

Hole size	<1/4 inch	1/4 to 1 inch	1 inch to full rupture
Expected failure rate	0.28×10^{-3}/mile/year	0.224×10^{-3}/mile/year	0.056×10^{-3}/mile/year

For pipelines from thirty to thirty-six inches in diameter:

Hole size	<1/4 inch	1/4 to 1 inch	1 inch to full rupture
Expected failure rate	0.10×10^{-3}/mile/year	0.08×10^{-3}/mile/year	0.02×10^{-3}/mile/year

QUEST

In the absence of applicable data, the injection pipelines in this study were assumed to have failure rates similar to the ones presented above for gas transmission pipelines. In addition, failure rates for the 3-inch pipeline were assumed to be similar to those of the 6-inch to 12-inch gas transmission pipelines.

4.7.2 Surface Equipment

Some types of pipeline equipment (such as pig launchers and receivers) are always located aboveground. In some instances, other types of pipeline equipment might also be located aboveground (e.g., block valves and blowdown valves). Failure rates for such equipment have been reported by Canada's Energy Resources Conservation Board [ERCB, 1990]. The reported rate for full-bore ruptures is 8.12×10^{-5} failures/equipment piece/year; and the reported rate for "leaks" is 2.95×10^{-4} failures/equipment piece/year.

Based on these data, the failure rates for surface equipment are expected to be as follows.

Hole size	<1/4 inch	1/4 to 1 inch	1 inch to full rupture
Expected failure rate	1.65×10^{-4}/piece/year	1.30×10^{-4}/piece/year	8.12×10^{-5}/piece/year

4.7.3 Emergency Shutdown Valves

The ERCB data base (ERCB, 1990) includes a failure rate for pipeline emergency shutdown valves of 1.17×10^{-2} failures per demand (i.e., an ESD valve is expected to fail to close once for every 85 times it is called upon to close).

4.8 Wellhead Failure Rates

The Energy Resources Conservation Board (ERCB) has compiled data on the frequency of accidental releases from completed wells in the province of Alberta, Canada [ERCB, 1990]. Based on these data, the frequency of well blowouts is expected to be 1.36×10^{-4} blowouts/well/year.

If a well is fitted with a subsurface safety valve (SSSV), a blowout of the well will not last more than a few seconds if the SSSV operates properly. According to ERCB data, the "fails to close" failure rate for SSSVs is 2.61×10^{-2} failures/demand (i.e., an SSSV is expected to fail about once every thirty-eight blowouts). Multiplying this failure rate by the frequency of well blowouts produces the frequency of uncontrolled well blowouts; 3.55×10^{-6}/well/year.

4.9 Common Cause Failures

Components that are exposed to a common working environment may be susceptible to common cause failures if they contain a common design error (e.g., wrong materials of construction specified) or a common manufacturing defect (e.g., improper welding technique). Thus, within a particular unit or facility, the failure rates of components, such as pipes, valves, pump seals, gaskets, etc., may be higher than the rates obtained from typical failure rate data bases, if the components are susceptible to common cause failures. However, common cause failures seldom exert a large influence on the actual failure rate of a specific type or class of component. Design reviews, quality control and quality assurance programs, process hazards analyses, accident investigations, etc., will generally reveal the sources of common cause failures either before such failures occur, or after only one or two such failures have occurred. The susceptible components are then respecified, repaired, or replaced, as required.

QUEST

Failures of sensing and control devices seldom lead directly to an accident. In most cases, the failure of such a device would lead to an accident only if other events occur simultaneously or sequentially. The contribution of such failures to the frequency of specific accidents can sometimes be estimated by techniques such as fault tree analysis. The presence of common cause failures in a fault tree will increase the complexity of the analysis.

In the analysis that is the subject of this report, each accident of interest involves the failure of a physical component of a process system. Available data bases for component failures include failures that occurred as the result of common causes. Hence, the expected frequencies of occurrence of the accidents of interest can be based directly on component failure rates obtained from historical data bases, and there is no need to resort to fault tree analysis or to adjust the estimated failure rates to account for common cause failures.

4.10   Human Error

The probability of occurrence of any specific accident can be influenced by human error. However, in most situations, it is not possible to quantify this influence. Fortunately, it is seldom necessary to attempt such quantification.

There are two general forms in which human error can contribute to the failure of a component or system of components. The first form, which is implicit in nature, includes poor component design, improper specification of components, flawed manufacturing, improper selection of materials of construction, and similar situations that result in the installation and use of defective components or the improper use of non-defective components. The second form, which is explicit in nature, includes improper operation and improper maintenance.

Most of the available equipment failure rate data bases do not categorize the causes of the failures. Whether the rupture of a pipe is due to excessive corrosion, poor design, improper welding procedure, or some other cause, the rupture is simply added to the data base as one "pipe failure." Thus, since implicit human errors manifest themselves in the form of component failures, they are already included in the failure rate data bases for component failures.

Many types of explicit human errors also manifest themselves in the form of component failures. Therefore, like implicit human errors, component failures caused by explicit human errors are already included in the failure rate data bases for component failures. For example, if a pump seal is improperly installed (improper maintenance) and it begins to leak after several hours of operation, it would simply be recorded in a failure rate data base as one "pump seal failure." Similarly, if an operator responds improperly (improper operation) to a high pressure alarm and the pressure continues to increase, ultimately resulting in the rupture of a pipe, the event is recorded in a failure rate data base as a "pipe rupture."

Except in rare cases, there is little reason to believe that equipment failures due to implicit or explicit human errors will occur more often or less often in a specific facility than in the facilities that contributed failure rate data to the data bases. Therefore, component failure rates obtained from historical data bases can nearly always be used without being modified to account for human error.

Accidents that are the result of explicit human errors, but do not involve failures of components, are not included in typical failure rate data bases. Examples of such accidents include overfilling a tank (resulting in a liquid spill), opening a flanged connection on a piping system that has not been properly drained and purged (resulting in a leak of gas or liquid), opening a water-draw-off valve on an LPG tank and then walking away (resulting in a release of LPG), etc.

QUEST

The contribution of explicit human error to the frequency of accidents that do not involve the failure of components can sometimes be estimated by techniques such as fault tree analysis or event tree analysis. These techniques are used to illustrate how the occurrence of an accident is the result of a chain of events or the simultaneous occurrence of several events. These events can be component failures or human failures. Using these techniques, the probability of occurrence of the accident can be quantified IF the probability of occurrence of EVERY event that contributes to the accident can be quantified. In many cases, there is insufficient historical data for some of the events. (This is particularly true for human error events.) Thus, assumed values must often be used. This inevitably leads to questions regarding the accuracy or applicability of the estimated probability of occurrence of the accident.

In the analysis that is the subject of this report, the accidents of interest all involve the failure of a physical component of a process system. Thus, frequencies of occurrence of these accidents (which are based on component failure rates obtained from historical data bases) need not be increased or decreased to account for human error.

4.11   Hazardous Events Following Fluid Releases

A release of hazardous fluid to the atmosphere may create one or more hazardous conditions, depending on events that occur subsequent to the release. For a fluid that is flammable and toxic, the possibilities are:

(a)   No ignition. If a flammable/toxic vapor cloud forms but never ignites, the only hazard is the toxicity of the cloud.

(b)   Immediate ignition. If ignition occurs nearly simultaneously with the beginning of the release, the hazard may be heat radiation from a torch fire (pressurized release) or pool fire (nonpressurized release).

(c)   Delayed ignition with no explosion. If there is a time delay between the start of the release and ignition of the release, a flammable/toxic vapor cloud will form. Before ignition, the cloud may present a toxic hazard. After ignition, there will be a vapor cloud fire (flash fire), possibly followed by a pool fire or torch fire.

(d)   Delayed ignition with explosion. This situation is identical to case (c), but subsequent to ignition the vapor cloud creates damaging overpressures due to accelerated combustion.

Each of these four possibilities has some probability of occurring, once a release has occurred. The sum of these four probabilities must equal one. The ignition/explosion probabilities employed in this study are taken from an Institution of Chemical Engineers report [IChemE, 1990]. Estimated values are a function of the "size" of the release.

Consequences of the hazardous events that may occur subsequent to a release of hazardous fluid are also proportional to the "size" of the release. Therefore, when calculating the accident probability, it is necessary to estimate the distribution of releases of various sizes. This is typically done by applying a hole size distribution, such as the one presented in Section 4.7.2 for pipeline surface equipment.

The estimates used for hole size and ignition probability are best illustrated by event trees, with a release of fluid as the initial event. One of the event trees prepared for this study is presented in Figure 4-1. It begins with the release of natural gas from a welded metal pipeline that has a nominal diameter of twelve inches. Moving from left to right, the tree first branches into three leak sizes, each being defined by the diameter (d) of the hole through which the fluid is being released. Each of these three branches divides into three branches based on ignition timing and probability. Each delayed ignition branch divides again into two branches: flash fire and vapor cloud explosion (VCE). At the far right of the event tree are the twelve "outcomes" that have some probability of occurring if the initiating release occurs. To arrive at the probability of a specific outcome, the overall failure rate is modified by the probability at each applicable branching of the event tree.

QUEST

The estimated annual probability of occurrence of each possible outcome, per meter of pipe, is listed on the event tree.

In general, small releases are the most likely to occur, the least likely to be ignited (small probability of reaching an ignition source), and least likely to result in vapor cloud explosions (insufficient mass of gas in the flammable gas cloud). The largest releases are the least likely to occur, the most likely to be ignited (highest probability of reaching an ignition source), the most likely to be ignited immediately (the force needed to cause a large release may also be capable of igniting the release), and the most likely to result in a vapor cloud explosion (highest probability of being partially confined by obstructions).

QUEST

Figure 4-1
Example Event Tree for a Flammable/Toxic Release

		Probability (Assuming Initiating Event Occurs)	Annual Probability per Mile of Pipeline	Outcome
Release from Natural Gas Pipeline				
Pipe Diameter 12 in				
(Annual Probability 1.52 x 10^{-3} mile/year)				
Rupture (10%) (1 in < d ≤ 12 in)	Immediate Ignition (10%)	0.010	1.52 x 10^{-5}	Torch Fire
	Delayed Ignition (20%) — Fire (90%)	0.018	2.74 x 10^{-5}	Flash Fire/Torch Fire
	Delayed Ignition (20%) — Vapor Cloud Explosion (10%)	0.002	3.03 x 10^{-6}	VCE
	No Ignition (70%)	0.070	1.06 x 10^{-4}	Toxic Cloud
Major Leak (40%) (0.25 in < d ≤ 1 in)	Immediate Ignition (2%)	0.008	1.22 x 10^{-5}	Torch Fire
	Delayed Ignition (5%) — Fire (95%)	0.019	2.89 x 10^{-5}	Flash Fire/Torch Fire
	Delayed Ignition (5%) — Vapor Cloud Explosion (5%)	0.001	1.52 x 10^{-6}	VCE
	No Ignition (93%)	0.372	5.65 x 10^{-4}	Toxic Cloud
Minor Leak (50%) (d ≤ 0.25 in)	Immediate Ignition (2%)	0.010	1.52 x 10^{-5}	Torch Fire
	Delayed Ignition (5%) — Fire (100%)	0.025	3.80 x 10^{-5}	Flash Fire/Torch Fire
	Delayed Ignition (5%) — Vapor Cloud Explosion (0%)	0.000	0.0	VCE
	No Ignition (93%)	0.465	7.07 x 10^{-4}	Toxic Cloud

QUEST

4-10

SECTION 5
RISK ANALYSIS METHODOLOGY

The Linam Ranch Plant, associated pipelines, proposed compressor(s), and proposed injection well pose no health hazards to the public as long as the equipment does not release flammable/toxic liquid or gas into the environment. In the event of an accident that results in a release of flammable/toxic material, persons near the release point may be at risk due to the properties of the vapor cloud created by the release.

The risk associated with the use of hazardous materials is often expressed as the product of the probability of occurrence of a hazardous event and the consequences of that event. Therefore, in order to quantify the risk associated with the transport, processing, compression, and injection of gas, it is necessary to quantify both the probability of releasing flammable/toxic material into the environment, and the consequences of such releases. The potential consequences of hazardous material releases include death or injury to persons near the release point.

5.1   Public/Industrial Risk Quantification

The methodology used in this study has been successfully employed in several QRA studies that have undergone regulatory review in countries worldwide. As an example, the following is a brief description of the steps involved in quantifying the risk to the public due to the natural gas transport and proposed reinjection options.

Conceptually, performing a risk analysis for the transport of toxic fluid is straightforward. For example, for releases of toxic materials, the analysis can be divided into the following steps. [Note that this comparative analysis only considers toxic materials. The flammable hazards common to all proposed options are not represented in this outline.]

Step 1. Within each "area" of the Linam Ranch Facility and along the pipeline routes, determine the potential credible releases that would create a toxic gas cloud.

Step 2. Determine the frequency of occurrence of each of these releases.

Step 3. Calculate the size of each potentially fatal hazard zone created by each of the releases identified in Step 1.
        i.   The hazard of interest is:
              a.   Toxic vapor clouds.
        ii.   The size of each hazard zone is a function of one or more of the following factors.
              a.   Orientation of the release.
              b.   Wind speed.
              c.   Atmospheric stability.
              d.   Local terrain (including diking and drainage).
              e.   Composition, pressure, and temperature of fluid being released.
              f.   Hole size.
              g.   Vessel inventories.
              h.   Diameter of liquid pool.

QUEST

Step 4. Determine the risk to the public in the vicinity of the facility.

i. For a specific wind direction, the potential exposure of any individual to a specific hazard zone depends on the following factors.

  a. Size (area) of the hazard zone.

  b. Location of the individual relative to the release location.

  c. Wind direction.

ii. Determine the exposure of the public to each potential hazard zone.

  a. Perform toxic vapor cloud hazard zone calculations for all wind directions, wind speeds, atmospheric stabilities, terrain conditions, and release orientations.

iii. Modify each of the above exposures by its probability of occurrence. Probabilities are divided into the following groups.

  a. P(wd,ws,stab) probability that the wind blows from a specified direction (wd), with a certain wind speed (ws), and a given atmospheric stability class, A through F (stab). Meteorological data are generally divided into sixteen wind directions, six wind speed classes, and six Pasquill-Gifford atmospheric stability categories. Although all 576 combinations of these conditions do not exist, a significant number will exist for each release studied. Figure 5-1 represents the wind speed versus stability distribution for the meteorological data (see Section 2.8).
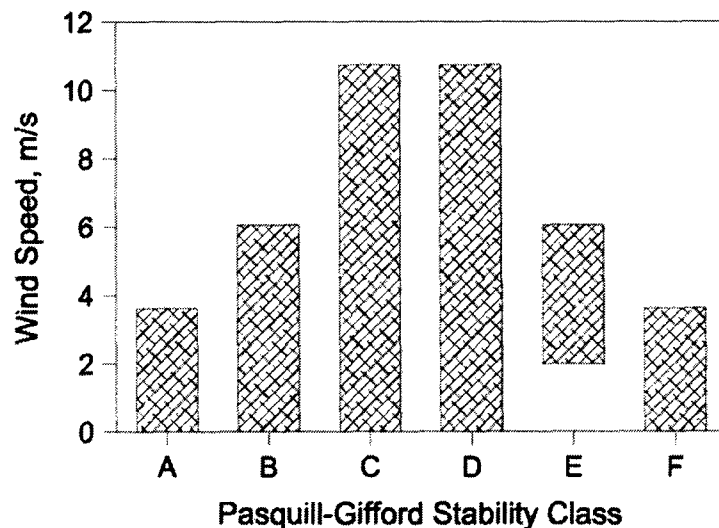

Figure 5-1
Wind Speed/Atmospheric Stability Categories for the
Hobbs, New Mexico Area

  b. P(acc) probability of occurrence of each accidental release identified in Step 1 (see Section 4).

  c. P(ii) probability of immediate ignition (i.e., probability that ignition occurs nearly simultaneously with the release) (see Section 4).

  d. P(di) probability of delayed ignition (i.e., probability that ignition occurs after a vapor cloud has formed) (see Section 4).

  e. P(vce) probability that the vapor cloud explodes following delayed ignition (see Section 4).

  f. P(orientation) probability that hazardous fluid is released into the atmosphere in a particular orientation.

QUEST

iv. Sum the potential exposures from each of the hazards for all releases identified in Step 1. This summation requires modifying each potential hazard zone by its probability of occurrence (i.e., the probability of a specific toxic vapor cloud is P(acc)*P(orientation) *P(ws,wd,stab)*(1-P(ii)-P(di)). Note that the probability of ignition remains in the calculation since it reduces the probability of generating a toxic gas cloud.

In this analysis, several simplifying assumptions were made to reduce the computation requirements and streamline the overall study. In each case, the simplifying assumption led to an <u>overprediction</u> of the potential risk to people outside the facility. These assumptions include:

(1) **Local terrain**. Although the terrain outside the facility or along the pipeline route is generally uniform, obstructions to vapor travel within the area are potentially significant. In this analysis, no additional dilution due to obstructions being in the travel path of the vapor cloud was taken into account. This assumption is applicable to all releases studied and results in an overprediction of the size of the potential hazard zones.

(2) **Meteorologic data**. The weather conditions (wind speed, atmospheric stability, and atmospheric temperature) existing at the time of a release all influence the dispersion of the released fluid. In this analysis, summer weather conditions were assumed for all releases. These conditions are "worst case" and provide for an overprediction of the annual potential risk.

The result of the analysis is a prediction of the toxic risk posed by the facility. Risk may be expressed in several forms (e.g., risk contours, average individual risk, societal risk, etc.). For this analysis, the focus was on the prediction of risk contours for exposure to hydrogen sulfide.

5.2   Risk Assessment

Risk indicators enable decision makers (i.e., corporate risk managers and regulatory authorities) to evaluate the risks associated with the reinjection options. The toxic risk contours for the Linam Gas Plant, pipeline segments, and injection well can be compared to each other as part of the risk assessment process.

QUEST

QUEST

SECTION 6
RISK ANALYSIS RESULTS AND CONCLUSIONS

This section presents a summary of the results of the risk analysis. These results are based on the consequence analysis presented in Section 3, the accident frequency analysis presented in Section 4, and the risk analysis methodology presented in Section 5. The analysis results are presented primarily in the form of risk contours.

6.1   Summary of Maximum Toxic Impact Zones

Differences in the toxic impact zones generated by potential releases from the various pipeline sections, sour gas treatment equipment, reinjection options, and wellhead are due primarily to differences in operating pressure, gas flow rates, and available inventory. In this study, the emphasis is on calculating the potential lethal exposure of the public to concentrations of H_2S or SO_2. For this reason, the toxic dispersion calculations were performed using probit relationships that account for time-varying effects. The 1% fatality probit level was used to define the maximum extent that a hazard may extend and cause a fatality (1% of the exposed population at the extent of the hazard). The 50% probit level was used to define a zone within which 50% of the exposed members of the public were assumed to be fatalities. The extent of the 99% probit hazard level defined a zone within which all of the exposed members of the public were assumed to be fatalities due to the release of gas containing H_2S or SO_2.

Table 6-1 presents a list of the fifteen accidental releases of toxic gas that generate the largest toxic impacts. The maximum predicted distances to the three mortality probit levels are listed for each release.

6.2   Measures of Risk Posed by Linam Ranch Pipelines, Sour Gas Treating Equipment, and Proposed Compression and Injection Well

Several different methods can be used to evaluate the risk of the Linam Ranch pipeline/compression/injection well system. Professionals in risk analysis recognize there is no single measure of risk that completely describes the risk a project poses to the public. Regulatory agencies have used methods such as hazard footprints, risk contours, f/N curves, and risk matrices to evaluate the risk posed by a project. This section of the report describes the risk measurement techniques that were applied to the Linam Ranch Gas Plant and, using each technique, evaluates the risk posed by each section of the system.

6.2.1   Linam Ranch Pipeline Hazard Footprints

A hazard footprint does not represent a true measure of the risk posed by a pipeline. The hazard footprint generally defines the maximum possible zone or area that could be affected by one or more accidents. The footprint will often be much larger than all but one single potential accident. This is the case for all of the Linam Ranch pipeline sections. For each pipeline section, a unique accident will generate the largest potentially fatal hazard zone along that pipeline route. For example, along the injection pipeline for AGI option #1, a full rupture of the line will create a toxic impact (defined by the 1% fatality H_2S probit) up to 1,435 feet away from the pipeline. No other potential accident will generate a hazard farther away than 1,435 feet from the pipeline.

QUEST

Release from	Distance [ft] from Release Point to Fatality Level		
	1%	50%	99%
Wellhead Tubing with SSSV Failure and Down-hole Check Valve Failure	4,185	3,300	2,595
Wellhead Tubing with SSSV Failure and Down-hole Check Valve Closure	1,815	1,550	1,315
3" Acid Gas Pipeline at AGI Wellsite (Option #1)	1,520	1,290	1,090
3" Acid Gas Pipeline (Option #1)	1,435	1,165	935
Acid Gas Compressor at AGI wellsite (Option #3)	1,410	1,150	930
Second Stage Acid Gas Compressor (Option #2)	1,400	1,145	920
Acid Gas Compressor at Gas Plant (Option #1)	1,380	1,125	910
18" Acid Gas Pipeline (Option #3)	1,150	940	760
8" Acid Gas Pipeline Aboveground (Option #2)	1,055	855	685
Acid Gas to SRU or Injection Pipeline	960	810	675
In-Plant Acid Gas Pipeline (Option #3)	940	790	655
8" Acid Gas Pipeline (Option #2)	675	480	*
First Stage Acid Gas Compressor (Option #2)	670	550	450
Reaction Furnace Outlet	465	370	260
Inlet Line to Converter #2	170	110	65

*Endpoint not reached at grade

Generating a continuous hazard footprint for the injection pipeline simply requires drawing a line parallel to the pipeline at a distance of 1,435 ft. An example of this type of hazard footprint, or more appropriately for a pipeline, a hazard corridor, is shown in Figure 6-1. It is important to note that the size of the hazard corridor is defined by the single worst possible accident.

A second precaution is necessary when reviewing hazard footprints. As stated above, the size of a potential impact resulting from an accidental release is generally much smaller than the defined maximum footprint. This is particularly true for pipeline hazard corridors. As seen in Figure 6-1, the area of the largest toxic impact zone defined by the 1% fatality H_2S probit is much smaller than the area contained within the hazard corridor along the route. The toxic impact zone outlined in Figure 6-1 (shown as the cross-hatched area) depicts the maximum possible area the toxic cloud might cover in the event of a full rupture, AND the wind blowing perpendicular to the pipeline, AND the wind speed is low, AND the atmosphere is calm. Thus, for the toxic impact zone to reach its maximum possible size, many different factors must be present during the course of the accident.

QUEST
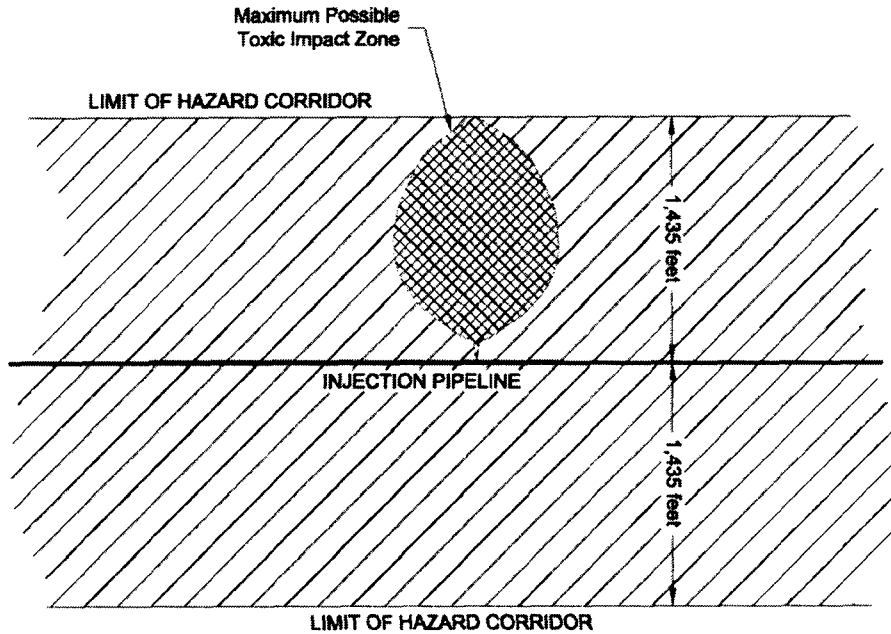
Figure 6-1
Maximum Hazard Corridor for the Injection Option #1 Pipeline

For these reasons, hazard footprints and corridors are not meaningful measures of the risk of a facility or pipeline. A hazard footprint simply provides information about which area could POTENTIALLY be exposed, but provides no information about the chances of exposure. Nevertheless, the maximum distances that define the toxic hazard corridors for the gas processing units, pipeline sections, and injection well are presented in Table 6-2.

Table 6-2
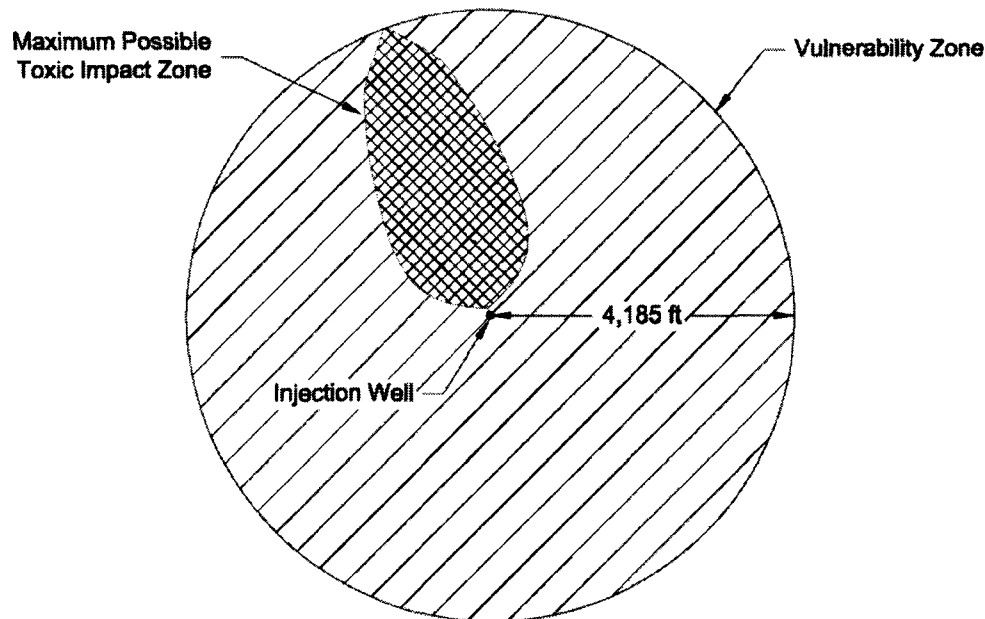**Maximum Toxic Hazard Footprint Lengths**

Equipment	Maximum Distance [ft] Defining Toxic Hazard Corridor
Buckeye Inlet Pipeline	30
Eddy Inlet Pipeline	12
Shell/Lea Inlet Pipeline	5
Injection Pipeline Option #1	1,435
Injection Pipeline Option #2	675
Injection Pipeline Option #3	1,150
Amine Unit Acid Gas	960
SRU Reaction Furnace Outlet	465
Wellhead	4,185

6-3

QUEST

6.2.2 Injection Well Site Hazard Footprints

Generating a toxic hazard footprint for equipment requires drawing a circle around the equipment. The radius of the circle is defined by the greatest distance achieved by a toxic impact.

As was the case with pipeline releases, the actual toxic impact zone from a unique accident will appear small in comparison to the total area that could potentially be covered by an accident that could occur. Figure 6-2 presents the maximum toxic zone for an injection well, as well as its vulnerability zone (the circle defining the outer limit of any release of gas).

Figure 6-2
Maximum Toxic Hazard Footprint for the Linam Injection Well

6.2.3 Risk Contours

Risk contours were constructed for the seven areas considered in this study:

- Buckeye, Eddy, and Shell/Lea inlet pipelines
- Inlet gas receiving and amine unit
- Sulfur recovery unit
- Acid gas injection option #1 – compression at Linam Ranch gas plant
- Acid gas injection option #2 – compression at Linam Ranch and at AGI wellsite
- Acid gas injection option #3 – compression at AGI wellsite.
- Acid gas injection wellsite

Risk contours present levels of risk based on annual exposure. For any risk level identified at a specific location, that level of risk is contingent upon one's presence 24 hours a day, 365 days per year. For this reason, risk contours do not describe the risk to populations that are inherently mobile, such as traffic on roadways or employees within a facility.

QUEST

The risk an individual is potentially exposed to by releases from the pipeline can be represented by a numerical measure. In this study, this numerical measure represents the chance or probability that an individual will be exposed to a fatal dose of hydrogen sulfide or sulfur dioxide during a year-long period, following a release from the Linam Ranch gas plant, injection pipelines, or injection well site. Table 6-3 lists the numerical value, the short-hand representation of that value as it is used in this report, and the value expressed in terms of chances per year.

Table 6-3
Risk Level Terminology and Numerical Values

Numerical Value	Shorthand Notation	Chance per Year of Fatality
1.0×10^{-4}/year	10^{-4}	One chance in 10,000 of being killed per year
1.0×10^{-5}/year	10^{-5}	One chance in 100,000 of being killed per year
1.0×10^{-6}/year	10^{-6}	One chance in 1,000,000 of being killed per year
1.0×10^{-7}/year	10^{-7}	One chance in 10,000,000 of being killed per year
1.0×10^{-8}/year	10^{-8}	One chance in 100,000,000 of being killed per year

6.2.3.1 Risk Contour Plots – Inlet Pipelines and Amine Unit

Toxic risk contours were developed for the three inlet pipelines, inlet receivers (slug catchers), and the sour gas treating amine unit. For the inlet pipelines, maximum risk for any of the three pipelines exists just above the pipeline. The actual risk associated with the three natural gas lines feeding the Linam Ranch Facility is dominated by the flammability of the gas. In all cases, the risk of fatality due to a failure, followed by ignition of the gas, is greater than the risk of exposure to H_2S. Because theis study based its comparison on toxic impacts only, the toxic risk from the inlet gas lines was found to be very small.

The inlet pipelines and amine treating unit are common to all of the four options being considered for the plant and were included in the risk contours for each option discussed below. It should be noted that none of the potential amine unit releases generate a large toxic impact when compared to the SRU or reinjection options (see Table 6-1).

6.2.3.2 Risk Contour Plots – Expanded Sulfur Recovery Unit

Risk contours were constructed for the sulfur recovery unit at the higher gas flowrate of 200 mmscfd. The extent of a specific risk level (e.g., 1.0×10^{-6}/yr, or one chance in one million per year of being exposed to a fatal hazard due to a release of toxic gas) is presented as a function of distance from the equipment.

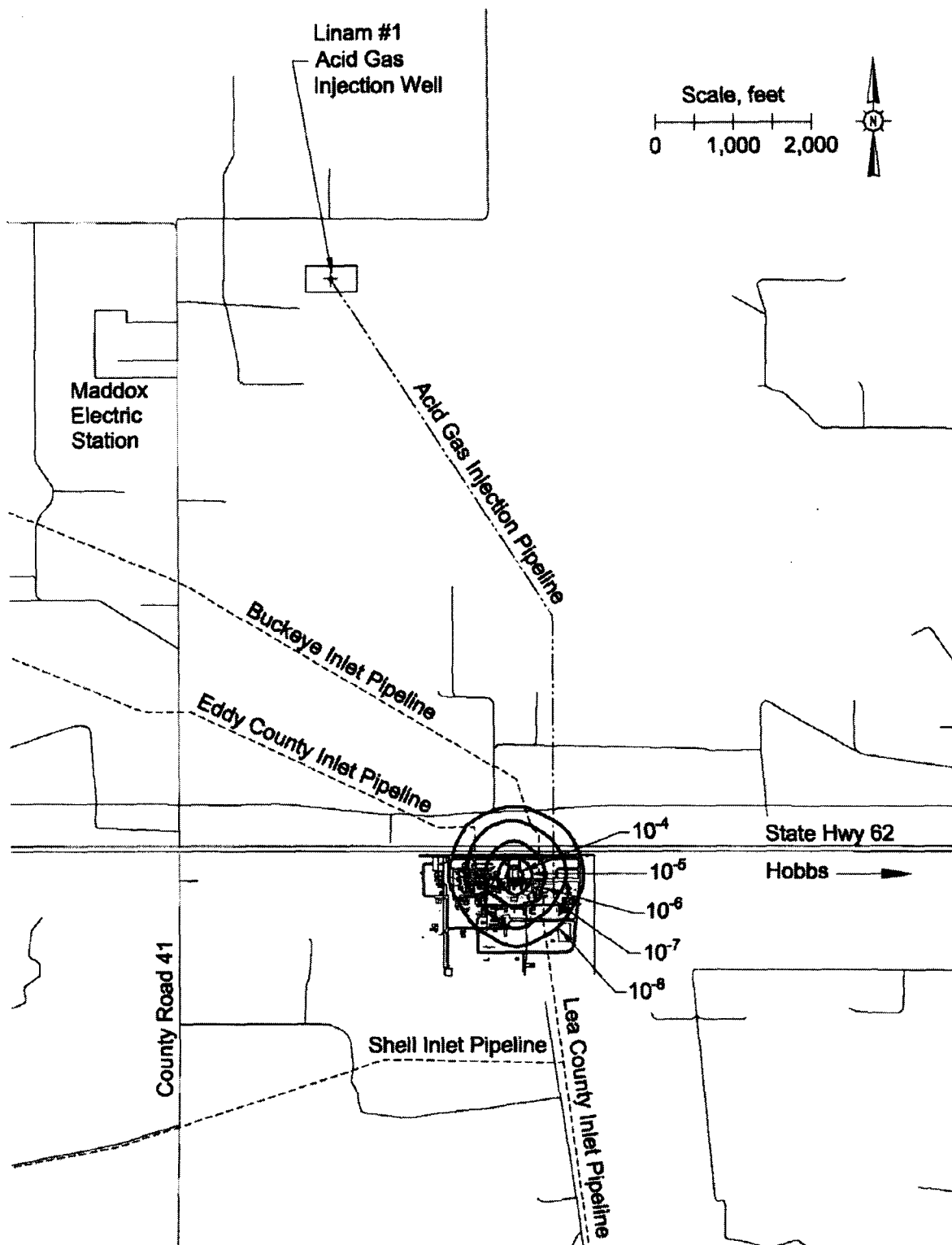As an example, the following information can be obtained from Figure 6-3, labeled "Sulfur Recovery Unit Risk Contours."

QUEST

Figure 6-3
Sulfur Recovery Unit Risk Contours

(a)   If an individual were continuously standing at the northern fenceline of the Linam Ranch Gas Plant for one year, he would have (at most) less than a 1.0×10^{-5}/yr (one in one hundred thousand per year) chance of being killed by a toxic cloud created by a release from the amine unit or SRU during that year. This is the risk level demonstrated by the 10^{-5} contour line shown in Figure 6-1. The release could be from any piece of equipment that resulted in a toxic vapor cloud.

(b)   If an individual were to continuously stand on State Highway 62 just outside the northern plant boundary for one year, his risk due to a toxic vapor cloud originating from the amine unit or SRU would be slightly higher than one in 1.0×10^{-6}/yr (one in one million per year) chance of being killed due to a toxic vapor cloud. This risk level is defined by the 10^{-6} line around the equipment in Figure 6-1.

6.2.3.3 Risk Levels – Compression and Reinjection Options

Plots of the risk levels surrounding the injection pipelines, compression equipment, and injection well site were constructed for the three reinjection options. For each option, the extent of a specific risk level is presented as a function of distance from the pipeline or wellhead.

Reinjection Option #1
Figure 6-4 presents the risk contours due to exposure to toxic gas for reinjection option #1, compression of the acid gas at the Linam Ranch gas plant. The risk corridor associated with the pipeline form the Linam Ranch plant to the AGI wellsite is approximately 900 feet wide to the 1.0×10^{-6}/yr level. The 1.0×10^{-6}/yr risk level extends up to 1,750 feet from the AGI wellsite.

Reinjection Option #2
Figure 6-5 presents the risk contours due to exposure to toxic gas for reinjection option #2, split compression of the acid gas at both the Linam Ranch gas plant and the injection wellsite. The maximum risk associated with the pipeline is approximately 6.5×10^{-8}/yr which closely follows the path of the pipeline between the Linam Ranch plant and the AGI wellsite and is significantly smaller than either options #1 or #3. The 1.0×10^{-6}/yr risk level extends up to 1,530 feet from the AGI wellsite.

Reinjection Option #3
Figure 6-6 presents the risk contours due to exposure to toxic gas for reinjection option #3, compression of the acid gas at the AGI wellsite. The maximum risk associated with the 18" acid gas pipeline is approximately 6.2×10^{-7}/yr. The 1.0×10^{-6}/yr risk level extends up to 1,500 feet from the AGI wellsite.

6.2.3.4 Risk Contour Summary

Risk contours are the most consistent way to compare the toxic risks posed by the various pipeline and equipment sections. Table 6-4 presents a summary of the extent of various risk levels as a function of distance away from the pipeline or facility for the equipment defined.

It is important to note that for the releases studied, the number of people in the area does not affect the calculation of risk contours. Thus, whether there are 1 or 100 people continuously standing 100 meters away from a pipeline or piece of equipment, each one's "risk" of exposure to toxic gas would be the same.
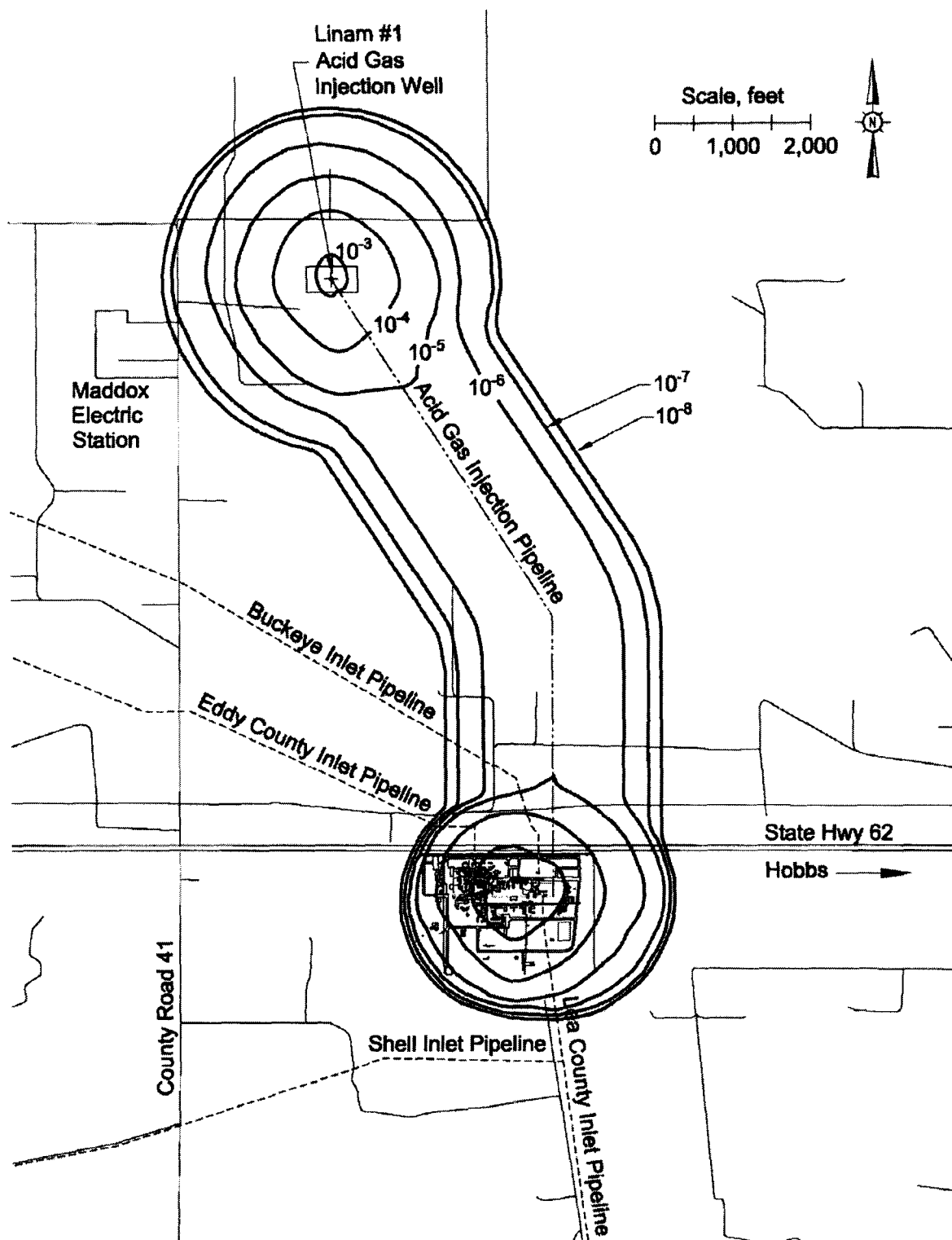
QUEST

Figure 6-4
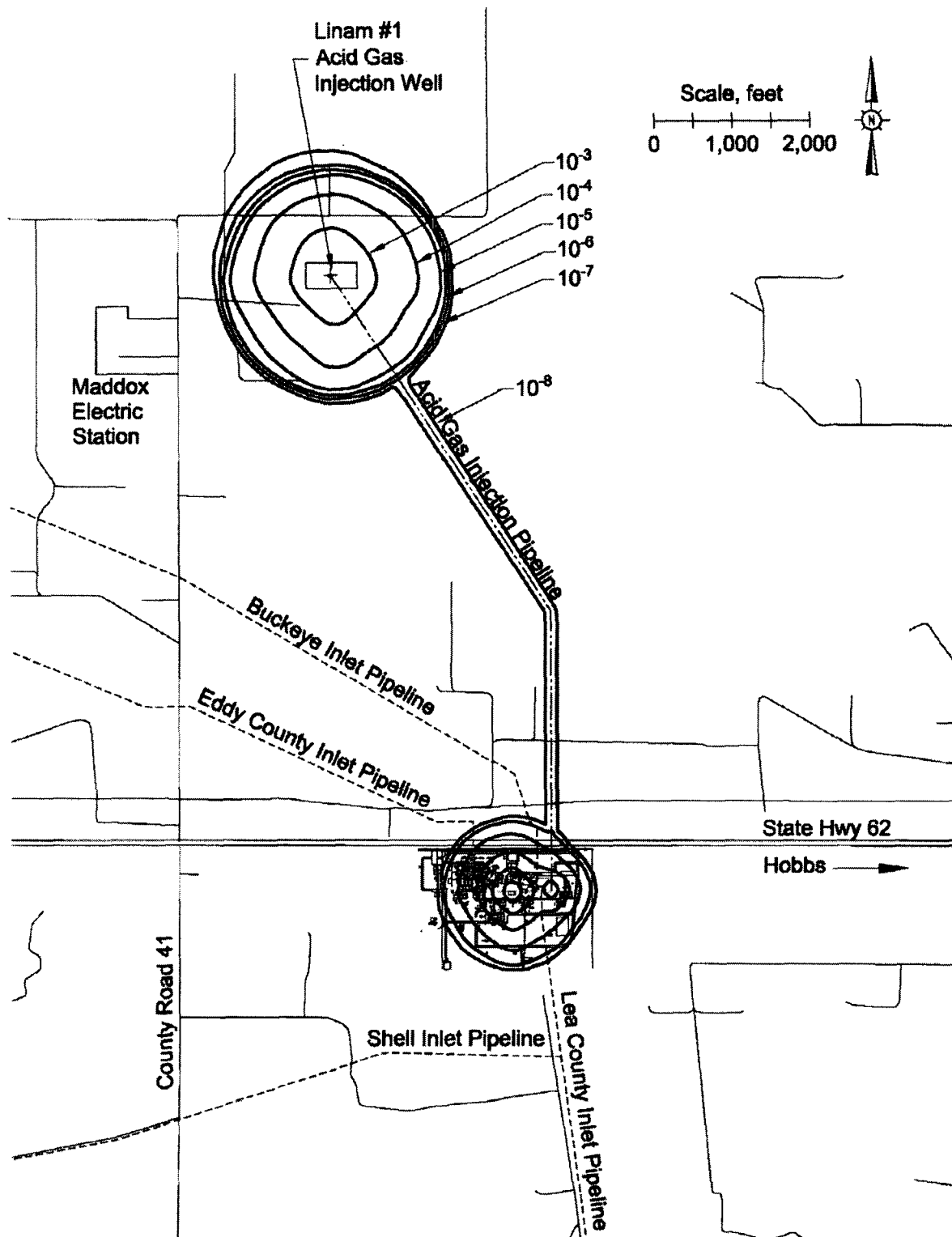**Reinjection Option #1 - Compression at Linam Ranch Risk Contours**

Linam #1
Acid Gas
Injection Well

10^{-3}
10^{-4}
10^{-5}
10^{-6}
10^{-7}
10^{-8}

Scale, feet

0   1,000   2,000

N

Maddox
Electric
Station

Acid Gas Injection Pipeline

Buckeye Inlet Pipeline

Eddy County Inlet Pipeline

State Hwy 62

Hobbs ⟶

County Road 41

Shell Inlet Pipeline

Lea County Inlet Pipeline

Figure 6-5
Reinjection Option #2 – Split Compression Risk Contours

QUEST
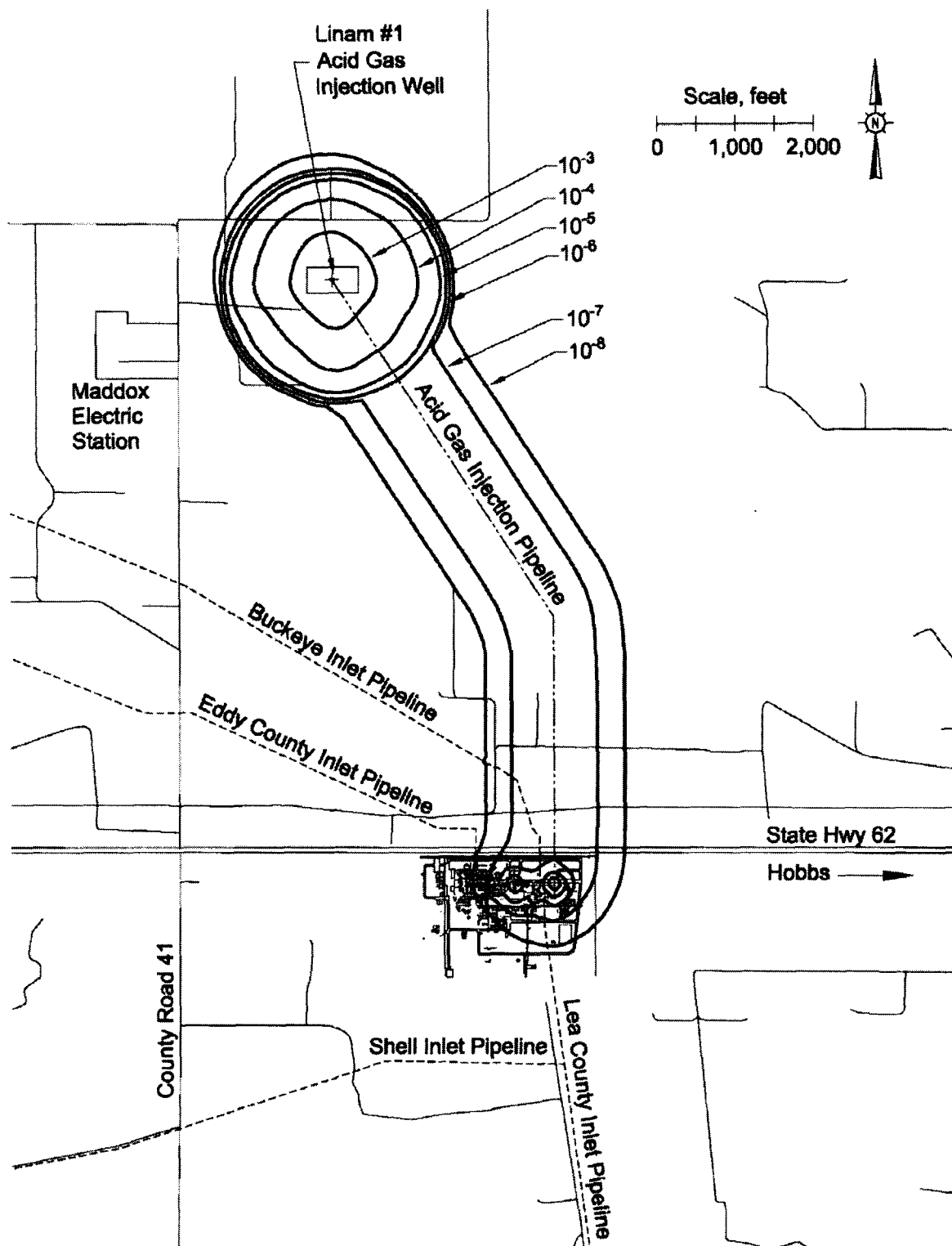
Figure 6-6
Reinjection Option #3 – Compression at AGI Wellsite Risk Contours

QUEST

Table 6-4
Distance to Risk Levels for Equipment Sections

Equipment Section	Maximum Distance [ft] to Specified Toxic Risk Levels				
	1.0×10^{-7}/yr	1.0×10^{-6}/yr	1.0×10^{-5}/yr	1.0×10^{-4}/yr	1.0×10^{-3}/yr
Sulfur Recovery Unit	700	425	250**	115**	DNE
Reinjection Option #1 - Pipeline	1,220	900	DNE	DNE	DNE
Reinjection Option #1 - Wellhead	2,100	1,750	1,500	900	300
Reinjection Option #2 - Pipeline	DNE	DNE	DNE	DNE	DNE
Reinjection Option #2 - Wellhead	1,560	1,530	1,450	1,170	630
Reinjection Option #3 - Pipeline	560	DNE	DNE	DNE	DNE
Reinjection Option #3 - Wellhead	1,550	1,500	1,435	1,130	615

DNE   Risk level does not exist around this section.
**   Risk level contained within facility boundaries.

QUEST

6.3   Evaluation of Risk Contours

Risk contour plots contain both the magnitude of a possible accident and the probability of occurrence of the accident. Each individual risk contour contains the toxic cloud shapes defined in the consequence portion of the analysis and the probability of occurrence of conditions that would allow these hazard zones to be created. In this manner, the maximum hazard distances that define the toxic clouds described earlier are matched with the probability that the rupture is complete, the gas does not ignite and the wind is blowing perpendicular to the pipeline.

The risk contour technique also considers potential releases that have little or no impact on the public. An example would be a small corrosion hole that releases gas into the soil and then the atmosphere on a day when the wind is blowing at 11 m/s (24 mph) under neutral (Pasquill D) atmospheric stability conditions. Such a release produces an impact zone of a few feet and poses little risk to the public.

The most consistent way to evaluate the risk posed to individuals in the vicinity of the Linam Ranch gas plant by each of the four acid gas treatment options is to compare the risk impacts for the different options. This method allows the reviewer to determine which option poses the greatest risk of toxic exposure, in terms of probability and magnitude, to people in the vicinity of the Linam Ranch gas plant. The risk contour plots for the different options were presented Figures 6-3 through 6-6, while Table 6-4 presented a summary of the risk results. From this information, it is clear that injection option #1, compression of the acid gas at the Linam Ranch gas plant, poses the greatest risk to people in the vicinity of the gas plant, injection pipeline, and injection well. From the analysis, the maximum fatal risk posed by the pipeline to an individual located directly above the pipeline is about 9.8×10^{-6} per year. In other words, an individual who remained above the 3-inch acid gas reinjection pipeline for an entire year would have one chance in about 102,000 of being fatally injured by a toxic gas cloud created by a release from the pipeline.

6.4   Study Conclusions

Quest Consultants Inc. performed a comparative risk analysis on Duke Energy's Linam Ranch gas plant acid gas treatment and reinjection options. The study was composed of three distinct tasks.

(1)   Quantifying the possible hazards posed by the gas pipelines, gas treatment equipment, sulfur recovery unit, compression options, and injection well.
(2)   Quantifying the potential failure rates for each of the hazardous events identified.
(3)   Combining the hazard zones and failure rates for each release to develop the risk of accidental exposure to toxic gas in the vicinity of the plant.

The first task, quantification of the hazard impacts posed by each equipment section, limits the overall analysis to areas within 4,185 feet of the injection wellhead. This was the maximum extent of the toxic hazard potentially created by a release from the wellhead tubing. Smaller distances were defined for other project components.

It is important to note that several conservative assumptions were made in the hazards identification section of this report (see Section 3). These assumptions forced the analysis to overpredict the extent of the toxic hazard zones.

The second task, calculation of accident frequencies, relied on historical data. Failure rates for surface equipment were taken from several accident and failure data bases. This information was presented in Section 4. Pipeline accident and well blowout frequencies relied on historical data available from the United States Department of Transportation and the Alberta Energy Resources Conservation Board.

QUEST

The average failure rate used in this report for a 3-inch pipeline is based on statistics compiled on pipelines with thinner walls than the high pressure pipeline that would be used in option #1. Thus, there is some uncertainty as to how this difference might affect the failure rate. It could be argued that the extra wall thickness would make it less likely for the pipeline to rupture when hit by a backhoe or other mechanized digging equipment, or that the extra wall thickness would reduce the likelihood of corrosion creating a hole in the pipe. However, there is no data that would quantitatively define how much the failure rate would be reduced. In addition, even if the failure rate of the 3-inch pipeline were decreased by a factor of 10 due to the thicker walls, this would simply cause the 1×10^{-6} individual risk contour along the pipeline in Figure 6-4 to become the 1×10^{-7} contour, and option #1 would still pose the greatest risk.

The third task undertaken in this work was the calculation of the risk posed to the public by the acid gas treatment options. In summary, the hazards and overall risks posed by the four acid gas treatment and reinjection options evaluated in this work are minimized with the expansion of the existing Sulfur Recovery Unit to treat the acid gas. Of the three injection options, option #2, the split compression option, results in the least risk to the exposed public.

To put the risk of the reinjection options in perspective, it is helpful to compare the predicted levels of risk to the risk of death from other sources. Table 6-5 lists several causes of early fatality by chance of fatality per year. Some probabilities associated with the reinjection options are included in the table for comparison.

QUEST

Table 6-5
Risk of Early Fatality by Various Causes

Hazard	Approximate Risk of Early Fatality, per Year	
	Probability	One Chance in
Heart disease[1]	2.32×10^{-3}	430
Cancer[1]	1.90×10^{-3}	526
All accidents[2]	5.70×10^{-4}	1,755
Motor vehicle (car, pickup, or van occupant)[2]	7.16×10^{-5}	13,960
Falls[2]	5.65×10^{-5}	17,710
Assault by firearm[2]	4.11×10^{-5}	24,340
Drowning[2]	1.20×10^{-5}	83,530
Motorcycle[2]	1.12×10^{-5}	89,560
Maximum risk from SRU at Linam Ranch Gas Plant northern fence line (no reinjection)	1.00×10^{-5}	100,000
Maximum risk from Linam Ranch AGI option #1, directly over the 3" acid gas pipeline	9.77×10^{-6}	102,300
Choking on food[2]	2.84×10^{-6}	351,600
Maximum risk from Linam Ranch AGI option #3, directly over the 18" acid gas pipeline	6.15×10^{-7}	1,626,000
Venomous animals and plants[2]	2.64×10^{-7}	3,788,700
Lightning[2]	2.29×10^{-7}	4,362,700
Bus accident (bus occupants)[2]	1.49×10^{-7}	6,696,300
Maximum risk from Linam Ranch AGI option #2, directly over the 8" acid gas pipeline	6.47×10^{-8}	15,456,000
Dog bites[2]	6.26×10^{-8}	15,966,734

[1] National Center for Health Statistics, "Deaths: Final Data for 2003", http://www.cdc.gov/nchs/data/hestat/finaldeaths03_tables.pdf, 2006.

[2] National Safety Council, "What are the Odds of Dying?", Statistics from 2002, http://www.nsc.org/lrs/statinfo/odds.htm, 2005.

QUEST

SECTION 7
REFERENCES

Bush, S. H. (1975), "Pressure Vessel Reliability." *Journal of Pressure Vessel Technology*, No. 97, Series J, February, 1975: pp. 54-70.

CCPS (1989), *Guidelines for Process Equipment Reliability Data, with Data Tables*. Center for Chemical Process Safety of the American Institute of Chemical Engineers, 345 East 47th Street, New York, New York 19917, 1989.

CCPS (1989), *Guidelines for Chemical Process Quantitative Risk Analysis*. Center for Chemical Process Safety of the American Institute of Chemical Engineers, 345 East 47th Street, New York, New York, 1989.

Chang, Joseph C., Mark E. Fernau, Joseph S. Scire, and David G. Strimaitis (1998), *A Critical Review of Four Types of Air Quality Models Pertinent to MMS Regulatory and Environmental Assessment Missions*. Mineral Management Service, Gulf of Mexico OCS Region, U.S. Department of the Interior, New Orleans, November, 1998.

DOT (1988), *Hazardous Materials Information System*. U.S. Department of Transportation, Materials Transportation Bureau, Washington, D.C., 1988.

E&P Forum (1992), *Hydrocarbon Leak and Ignition Data Base*. The Oil Industry International Exploration and Production Forum, Report No. 11.4/180, London, United Kingdom, May, 1992.

EGPIDG (1988), *Gas Pipeline Incidents*. A report of the European Gas Pipeline Incident Data Group, April, 1988.

ERCB (1990), *Risk Approach: An Approach for Estimating Risk to Public Safety from Uncontrolled Sour Gas Releases* (Volume 6). Energy Resources Conservation Board, Report 90-B, Calgary, Alberta, Canada, October, 1990.

Fearnehough, G. D. (1985), "The Control of Risk in Gas Transmission Pipelines." Presented at the *Institution of Chemical Engineers Symposium on Assessment and Control of Major Hazards*, Manchester, United Kingdom, April, 1985

Green, A. E., and A. J. Bourne (1972), *Reliability Technology*. John Wiley and Sons, Ltd., New York, New York, 1972.

Hanna, S. R., D. G. Strimaitis, and J. C. Chang (1991), "Uncertainties in Hazardous Gas Model Predictions". *International Conference and Workshop on Modeling and Mitigating the Consequences of Accidental Releases of Hazardous Materials*, Center for Chemical Process Safety of the American Institute of Chemical Engineers, New Orleans, Louisiana, May 20-24, 1991

HSE (1991), *Major Hazard Aspects of the Transport of Dangerous Substances*. Health and Safety Executive, Advisory Committee on Dangerous Substances, London, United Kingdom, 1991.

IChemE (1990), A. W. Cox, F. P. Lees, and M. L. Ang, *Classification of Hazardous Locations*. The Institution of Chemical Engineers, 1990.

QUEST

Jones, D. J., G. S. Kramer, D. N. Gideon, and R. J. Eiber (1986), *An Analysis of Reportable Incidents for Natural Gas Transmission and Gathering Lines, 1970 through June 1984*. Prepared for the Pipeline Research Committee, American Gas Association, NG-18, Report No. 158, March, 1986.

OREDA (1984), *OREDA, Offshore Reliability Data Handbook* (First Edition). OREDA, Post Office Box 370, N-1322 Hovik, Norway, 1984.

Smith, T. A., and R. G. Warwick (1981), *A Survey of Defects in Pressure Vessels in the United Kingdom for the Period 1962-1978 and Its Relevance to Nuclear Primary Circuits*. Safety and Reliability Directorate, SRD R-203, United Kingdom Atomic Energy Authority, December, 1981.

Sooby, W., and J. M. Tolchard (1993), "Estimation of Cold Failure Frequency of LPG Tanks in Europe." Paper presented at the *Conference on Risk and Safety Management in the Gas Industry*, Hong Kong, October, 1993.

Stiver, W., and D. Macay (1983), "Evaporation Rates of Chemical Spills." *Environment Canada First Technical Spills Seminar*, Toronto, Canada, 1983.

TRC (1991), *Evaluation of Dense Gas Simulation Models*. Prepared for the U.S. Environmental Protection Agency by TRC Environmental Consultants, Inc., East Hartford, Connecticut, 06108, EPA Contract No. 68-02-4399, May, 1991.

Tsao, C. K., and W. W. Perry (1979), *Modifications to the Vulnerability Model: A Simulation System for Assessing Damage Resulting from Marine Spills*. U.S. Coast Guard Report CG-D-38-79, Washington, D.C., March, 1979.

USNRC (1975), *Reactor Safety Study: An Assessment of Accident Risks in U.S. Commercial Nuclear Power Plants*. WASH 1400, U.S. Nuclear Regulatory Commission, Washington, D.C., October, 1975.

QUEST

APPENDIX A
CANARY BY QUEST® MODEL DESCRIPTIONS

The following model descriptions are taken from the **CANARY** by Quest User Manual.

QUEST

Engineering Properties

Purpose

The purpose of this model is to provide an accurate means of computing physical and thermodynamic properties of a wide range of chemical mixtures and pure components using a minimum of initial information.

Required Data

(a)   Fluid composition
(b)   Temperature and pressure of the fluid prior to release

Methodology

Basic thermodynamic properties are computed using the Peng-Robinson equation of state [Peng and Robinson, 1976]. The necessary physical and thermodynamic properties are calculated in the following manner.

Step 1: The temperature and pressure of the fluid at storage conditions and the identity and mole fraction of each component of the fluid are obtained. Mixture parameters are determined using data from the extensive properties data base within CANARY.

Step 2: Each calculation begins with the computation of the vapor and liquid fluid composition. For cases where the temperature and pressure result in only one phase being present, the vapor or liquid composition will be the same as the initial feed composition. The composition calculation is an iterative procedure using a modification of the techniques described by Starling [1973].

Step 3: Once the vapor and liquid compositions are known, the vapor and liquid densities, enthalpies, entropies, and heat capacities can be computed directly. Other physical properties (viscosity, thermal conductivity, surface tension, etc.) are computed using correlations developed in Reid, Prausnitz, and Poling [1987].

Step 4: A matrix of properties is computed over a range of temperatures and pressures. Physical and thermodynamics properties required by other models within CANARY are then interpolated from this table.

Basic Thermodynamic Equations

$$Z^3 - (1-B) \cdot Z^2 + \left(A - 3 \cdot B^2 - 2 \cdot B\right) \cdot Z - \left(A \cdot B - B^2 - B^3\right) = 0 \tag{1}$$

where: Z = fluid compressibility factor, $\dfrac{P \cdot V}{R \cdot T}$, dimensionless

P = system pressure, kPa

V = fluid specific volume, m³/kmol

R = gas constant, $8.314 \ m^3 \cdot kPa/(kmol \cdot K)$

T = absolute temperature, K

$A \ = \dfrac{a \cdot P}{R^2 \cdot T^2}$

$a \ = 0.45724 \cdot \dfrac{R^2 \cdot T^2}{P_c} \cdot \alpha$

$\alpha \ = \left[1 + m \cdot \left(1 - T_r^{0.5} \right)^2 \right]$

$m \ = 0.37464 + 1.54226 \cdot \omega - 0.26992 \cdot \omega^2$

ω = acentric factor

$T_r \ = \dfrac{T}{T_c}$

T_c = pseudo-critical temperature, K

P_c = pseudo-critical pressure, kPa

$B \ = \dfrac{b \cdot P}{R \cdot T}$

$b \ = 0.0778 \cdot R \cdot \dfrac{T_c}{P_c}$

$$H = H^o + \frac{P}{\rho} - R \cdot T + \int_0^\rho \left[P - T \cdot \left(\frac{\partial P}{\partial T} \right)_\rho \right] \cdot \left(\frac{d\rho}{\rho^2} \right) \qquad (2)$$

where: H = enthalpy of fluid at system conditions, kJ/kg

H^o = enthalpy of ideal gas at system temperature, kJ/kg

$$S = S^o - R \cdot \ln \left(\rho \cdot R \cdot T \right) + \int_0^\rho \left[\rho \cdot R - \left(\frac{\partial P}{\partial T} \right)_\rho \right] \cdot \left(\frac{d\rho}{\rho^2} \right) \qquad (3)$$

where: S = entropy of fluid at system conditions, kJ/(kg$\cdot$K)

S^o = entropy of ideal gas at system temperature, kJ/(kg$\cdot$K)

$$R \cdot T \cdot \ln \left(\frac{f_i}{f_i^o} \right) = \left[\left(H_i - H_i^o \right) - T \cdot \left(S_i - S_i^o \right) \right] \qquad (4)$$

where: f_i = fugacity of component i, kPa

f_i^o = standard state reference fugacity, kPa

References

Peng, D., and D. B. Robinson, "New Two-Constant Equation of State." *Industrial Engineering Chemistry Fundamentals*, Vol. 15, No. 59, 1976.

Reid, R. C., J. M. Prausnitz, and B. E. Poling, *The Properties of Gases and Liquids* (Fourth Edition). McGraw-Hill Book Company, New York, New York, 1987.

Starling, K. E., *Fluid Thermodynamic Properties for Light Petroleum Systems*. Gulf Publishing Company, Houston, Texas, 1973.

Fluid Release Model

Purpose

The purpose of the Fluid Release Model is to predict the rate of mass release from a breach of containment. Specifically, the model predicts the rate of flow and the physical state (liquid, two-phase, or gas) of the release of a fluid stream as it enters the atmosphere from a circular breach in a pipe or vessel wall. The model also computes the amount of vapor and aerosol produced and the rate at which liquid reaches the ground.

Required Data

(a)   Composition of the fluid
(b)   Temperature and pressure of the fluid just prior to the time of the breach
(c)   Normal flow rate of fluid into the vessel or in the pipe
(d)   Size of the pipe and/or vessel
(e)   Length of pipe
(f)   Area of the breach
(g)   Angle of release relative to horizontal
(h)   Elevation of release point above grade

Methodology

Step 1: Calculation of Initial Flow Conditions

The initial conditions (before the breach occurs) in the piping and/or vessel are determined from the input data, coupled with a calculation to determine the initial pressure profile in the piping. The pressure profile is computed by dividing the pipe into small incremental lengths and computing the flow conditions stepwise from the vessel to the breach point. As the flow conditions are computed, the time required for a sonic wave to traverse each section is also computed. The flow in any length increment can be all vapor, all liquid, or two-phase (this implies that the sonic velocity within each section may vary). As flow conditions are computed in each length increment, checks are made to determine if the fluid velocity has exceeded the sonic velocity or if the pressure in the flow increment has reached atmospheric. If either condition has been reached, an error code is generated and computations are stopped.

Step 2: Initial Unsteady State Flow Calculations

When a breach occurs in a system with piping, a disturbance in flow and pressure propagates from the breach point at the local sonic velocity of the fluid. During the time required for the disturbance to reach the upstream end of the piping, a period of highly unsteady flow occurs. The portion of the piping that has experienced the passage of the pressure disturbance is in accelerated flow, while the portion upstream of the disturbance is in the same flow regime as before the breach occurred.

To compute the flow rate from the breach during the initial unsteady flow period, a small time increment is selected and the distance that the pressure disturbance has moved in that time increment is computed using the sonic velocity profile found in the initial pressure profile calculation. The disturbed length is subdivided into small increments for use in an iterative pressure balance

calculation. A pressure balance is achieved when a breach pressure is found that balances the flow from the breach and the flow in the disturbed section of piping. Another time increment is added, and the iterative procedure continues. The unsteady period continues until the pressure disturbance reaches the upstream end of the pipe.

Step 3: Long-Term Unsteady State Flow Calculations

The long-term unsteady state flow calculations are characterized by flow in the piping system that is changing more slowly than during the initial unsteady state calculations. The length of accelerated flow in the piping is constant, set by the user input pipe length. The vessel contents are being depleted, resulting in a potential lowering of pressure in the vessel. As with the other flow calculations, the time is incremented and the vessel conditions are computed. The new vessel conditions serve as input for the pressure drop calculations in the pipe. When a breach pressure is computed that balances the breach flow with the flow in the piping, a solution for that time is achieved. The solution continues until the ending time or other ending conditions are reached.

The frictional losses in the piping system are computed using the equation:

$$h = \left(\frac{4 \cdot f \cdot L \cdot U_{ls}^2}{2 \cdot g_c \cdot D_e} \right) \tag{1}$$

where: h = head (pressure) loss, ft of fluid
f = friction factor
L = length of system, ft
U = average flowing velocity, ft/sec
g_c = gravitational constant, 32.2 $lb_m \cdot ft/(lb_f \cdot sec^2)$
D_e = equivalent diameter of duct, ft

The friction factor is computed using the following equation:

$$\frac{1}{\sqrt{f}} = 1.74 - 2.0 \cdot \log_{10}\left[\frac{2 \cdot \varepsilon}{D_e} + \frac{18.7}{Re \cdot \sqrt{f}} \right] \tag{2}$$

where: ε = pipe roughness, ft
Re = Reynolds number, $D_e \cdot U \cdot \rho / \mu$, dimensionless
ρ = fluid density, lb/ft³
μ = fluid viscosity, lb/(ft·sec)

Equations (1) and (2) are used for liquid, vapor, and two-phase flow regimes. Since the piping is subdivided into small lengths, changes in velocity and physical properties across each segment are assumed to be negligible. At each step in the calculation, a check is made to determine if the fluid velocity has reached or exceeded the computed critical (sonic) velocity for the fluid. If the critical velocity has been exceeded, the velocity is constrained to the critical velocity and the maximum mass flow rate in the piping has been set.

If the fluid in the piping is in two-phase flow, the Lockhart and Martinelli [1949] modification to Equation (1) is used. The Lockhart and Martinelli equation for head loss is shown below:

$$h_{TP} = \Phi^2 \cdot \left(\frac{4 \cdot f \cdot L \cdot U_{ls}^2}{2 \cdot g_c \cdot D_e} \right) \tag{3}$$

where: h_{TP} = head loss for two-phase flow, ft of fluid

Φ = empirical parameter correlating single- and two-phase flow, dimensionless

U_{ls} = superficial liquid velocity (velocity of liquid if liquid filled the pipe), ft/sec

This equation is valid over short distances where the flowing velocity does not change appreciably.

Validation

Validation of fluid flow models is difficult since little data are available for comparison. Fletcher [1983] presented a set of data for flashing CFC-11 flowing through orifices and piping. Figures E-1 through E-4 compare calculations made using the Fluid Release Model with the data presented by Fletcher. Figure E-1 compares fluid fluxes for orifice type releases. These releases had length-to-diameter (L/D) ratios less than 0.88. Figure E-2 compares computed and experimental release fluxes for an L/D ratio of 120 at several levels of storage pressure. Figure E-3 compares similar releases for an L/D of 37.5. Figure E-4 shows predicted and experimental release fluxes at a given pressure for L/D ratios from 1 to 200.

Figures E-5 and E-6 compare computed and experimental gas discharge rates for the complete breach of two pipes. One pipe had an internal diameter of 6.2 inches (0.157 m); the other had a diameter of 12 inches (0.305 m). These pipes were initially pressurized to 1,000 psia with air and then explosively ruptured. The experimental values were reported in a research paper for Alberta Environment, authored by Wilson [1981].

Aerosols and Liquid Droplet Evaporation

Liquids stored at temperatures above their atmospheric pressure boiling point (superheated liquids) will give off vapor when released from storage. If the temperature of storage is sufficiently above the normal boiling point, the energy of the released vapor will break the liquid stream into small droplets. If these droplets are small enough, they will not settle, but remain in the vapor stream as aerosol droplets. The presence of aerosol droplets in the vapor stream changes its apparent density and provides an additional source of vapor. Droplets large enough to fall to the ground will lose mass due to evaporation during their fall.

The prediction of aerosol formation and amount of aerosol formed is based on the theoretical work performed for the Center for Chemical Process Safety (CCPS) by CREARE. CREARE's work has been extended and corrected by Quest. The extension to the model computes the non-aerosol drop evaporation. In Figure E-7, the four experimental data sets available for comparison (chlorine (Cl_2), methylamine (MMA), CFC-11, and cyclohexane) are compared to the values computed by the **CANARY** Aerosol Model.
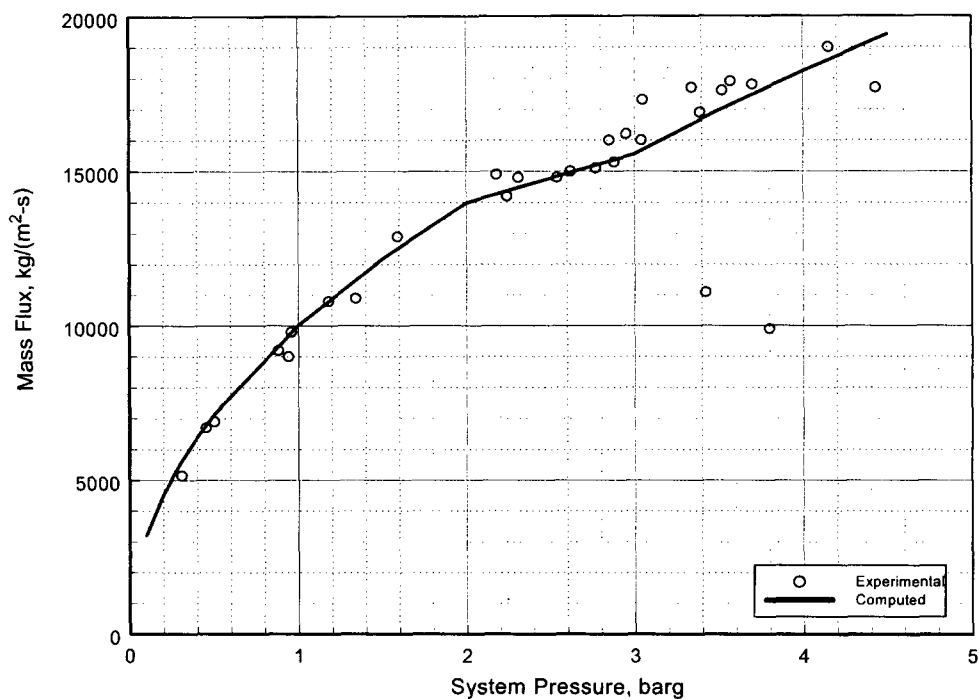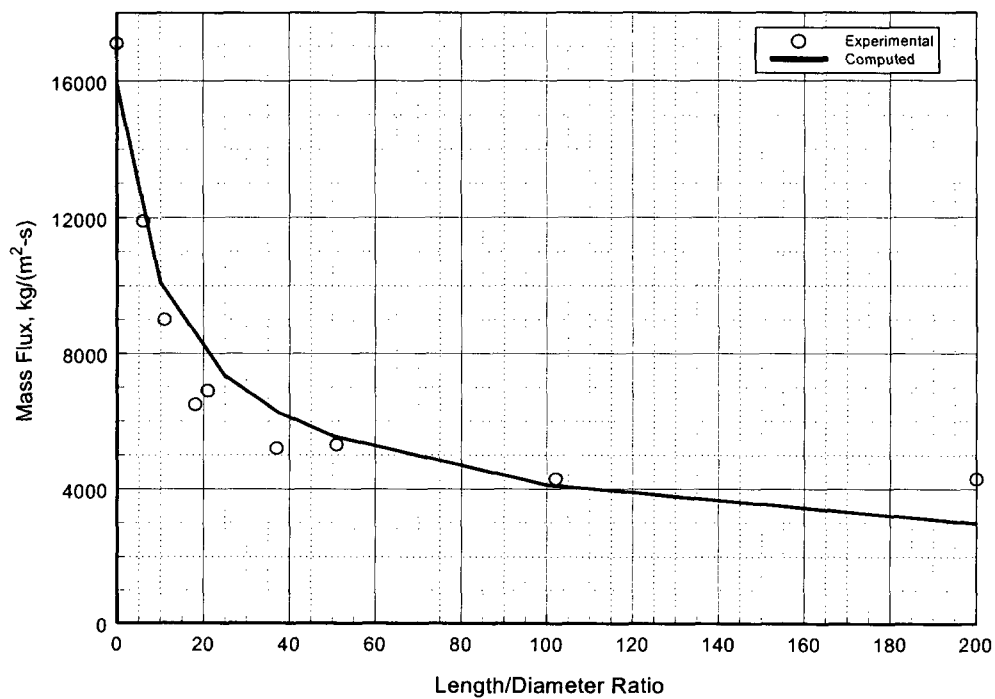
Figure E-1
Comparison of CFC-11 Orifice Releases as a Function of System Pressure
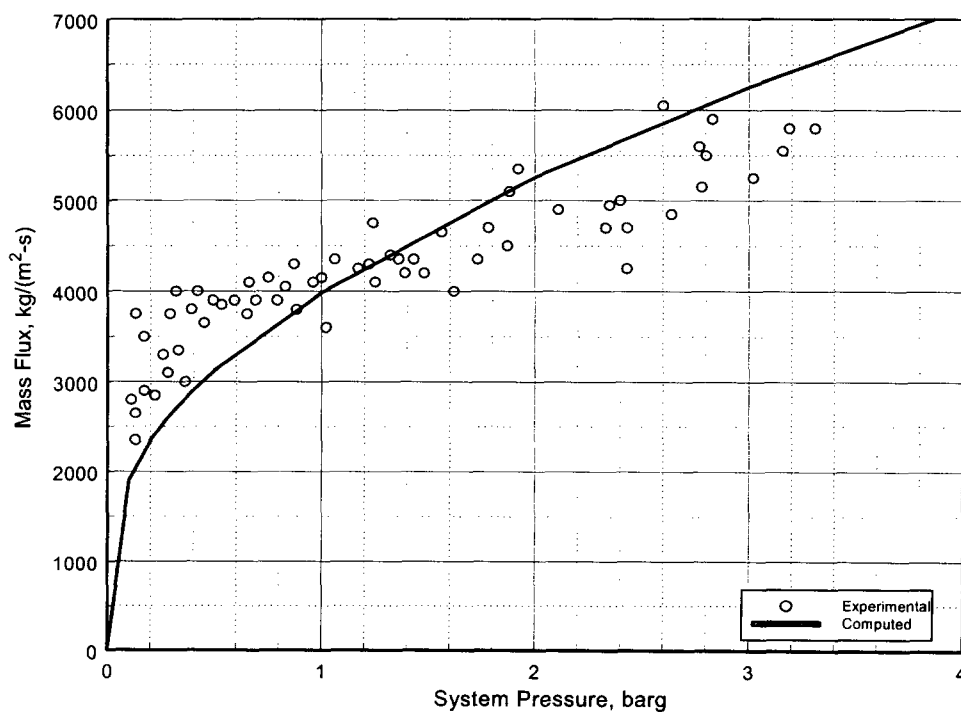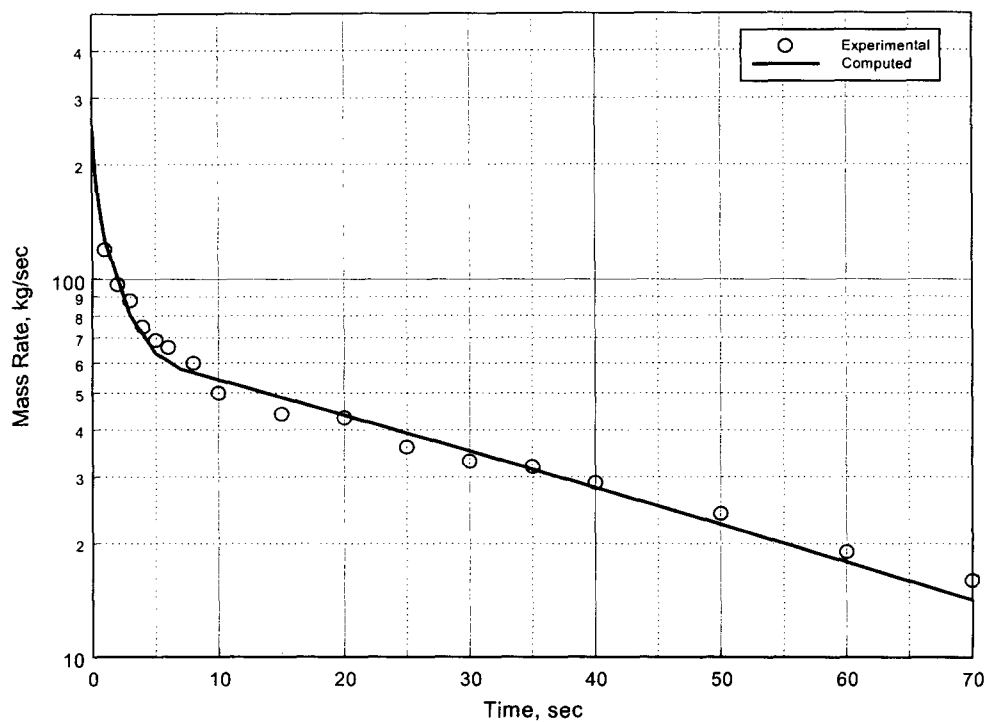

Figure E-2
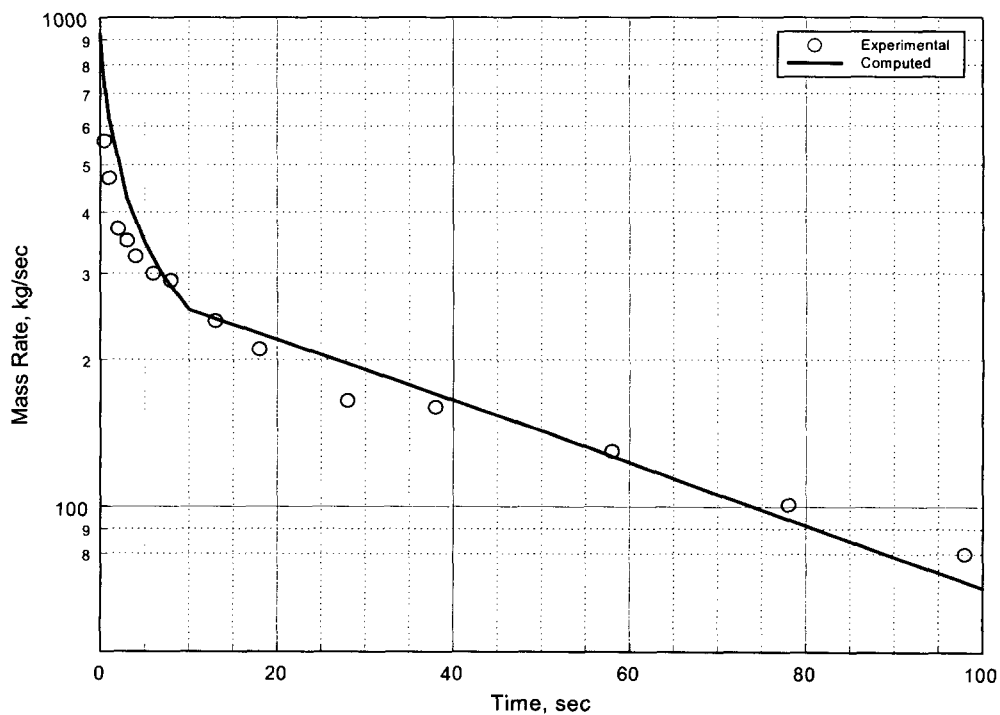**CFC-11 Release Rate Comparison with L/D of 120**
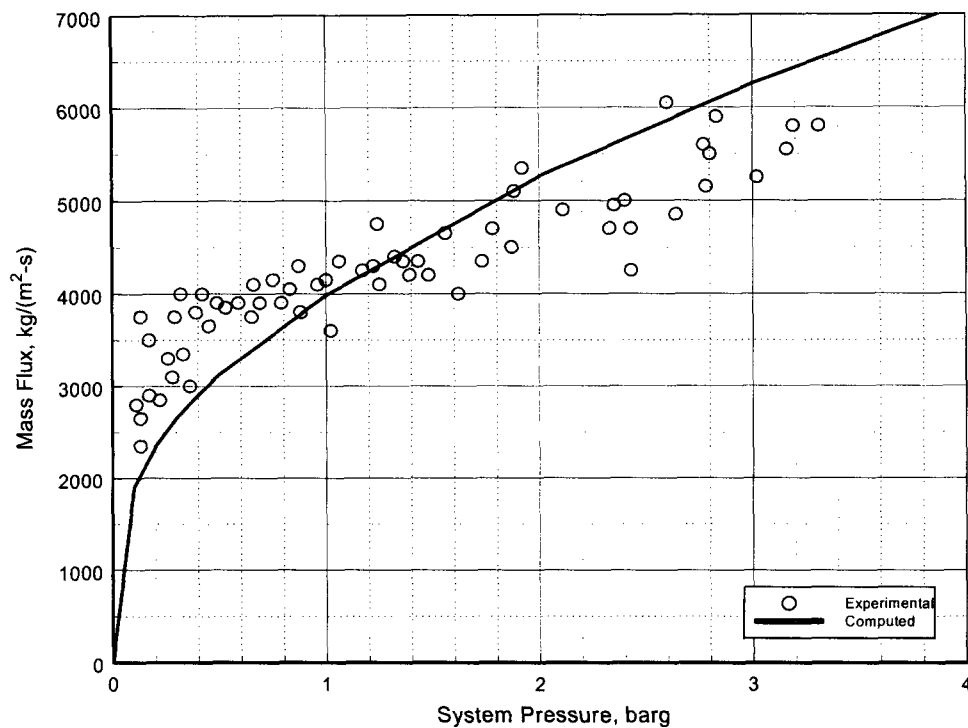
Figure E-3
CFC-11 Release Rate Comparison with L/D of 37.5
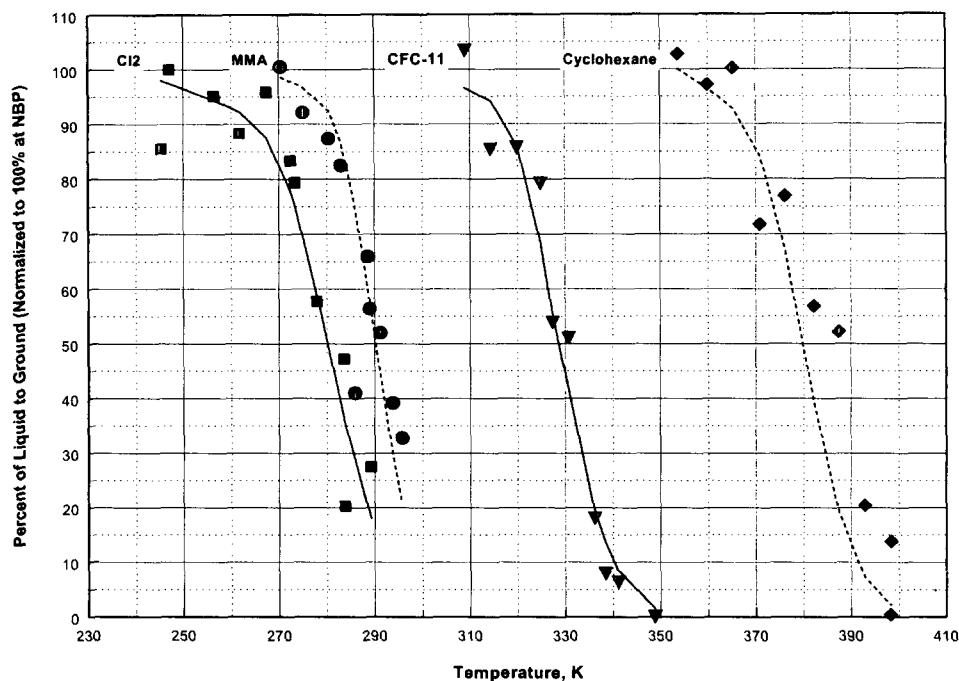

Figure E-4
CFC-11 Release Rate Comparison at Varying L/D Ratios

Figure E-5
Air Discharge Rates for 0.157 m Diameter Piping

Figure E-6
Air Discharge Rates for 0.305 m Diameter Piping

Figure E-7
Aerosol Formation as a Function of Storage Temperature

References

Fletcher, B., "Flashing Flow Through Orifices and Pipes." Paper presented at the AIChE Loss Prevention Symposium, Denver, Colorado, 1983.

Lockhart, R. W., and R. C. Martinelli, "Proposed Correlation of Data for Isothermal Two-Phase, Two-Component Flow in Pipes." Chemical Engineering Progress, Vol. 45, 1949: p. 39.

Wilson, D. J., "Expansion and Plume Rise of Gas Jets from High Pressure Pipeline Ruptures." Research Paper, Pollution Control Division, Alberta Environment, April, 1981.

Momentum Jet Dispersion Model

Purpose

The purpose of this model is to predict the dispersion of a jet release into ambient air. It is used to predict the downwind travel of a flammable or toxic gas or aerosol momentum jet release.

Required Data

(a)   Composition and properties of the released material
(b)   Temperature of released material
(c)   Release rate of material
(d)   Vertical release angle relative to wind direction
(e)   Height of release
(f)   Release area
(g)   Ambient wind speed
(h)   Ambient Pasquill-Gifford stability class
(i)   Ambient temperature
(j)   Relative humidity
(k)   Surface roughness scale

Methodology

Step 1: An assumption is made that flow perpendicular to the main flow in the plume is negligible, that the velocity and concentration profiles in the jet are similar at all sections of the jet, that molecular transport in the jet is negligible, and that longitudinal turbulent transport is negligible when compared to longitudinal convective transport. The coordinate system is then defined in s and r, where s is the path length of the plume and r is the radial distance from the plume centerline. The angle between the plume axis and horizontal is referred to as θ. Relationships between the downwind coordinate, x, vertical coordinate, y, and plume axis are given simply by:

$$\frac{dx}{ds} = \cos(\theta) \tag{1}$$

and

$$\frac{dy}{ds} = \sin(\theta) \tag{2}$$

Step 2: Velocity, concentration, and density profiles are assumed to be cylindrically symmetric about the plume axis and are assumed to be Gaussian in shape. The three profiles are taken as:

$$u(s,r,\theta) = U_a \cdot \cos(\theta) + u^*(s) \cdot e^{\frac{-r^2}{b^2(s)}} \tag{3}$$

where: u = plume velocity, m/s

U_a = ambient wind speed, m/s

u^* = plume velocity relative to the wind in the downwind direction at the plume axis, m/s

$b(s)$ = characteristic width of the plume at distance s from the release, m

$$\rho(s,r,\theta) = \rho_a + \rho^*(s) \cdot e^{\frac{-r^2}{\lambda^2 \cdot b^2(s)}} \tag{4}$$

where: ρ = plume density, kg/m³

ρ_a = density of ambient air, kg/m³

$\rho^*(s)$ = density difference between plume axis and ambient air, kg/m³

λ^2 = turbulent Schmidt number, 1.35

$$c(s,r,\theta) = c^*(s) \cdot e^{\frac{-r^2}{\lambda^2 \cdot b^2(s)}} \tag{5}$$

where: c = pollutant concentration in the plume, kg/m³

$c^*(s)$ = pollutant concentration at plume centerline, kg/m³

Step 3: The equation for air entrainment into the plume and the conservation equations can then be solved. The equation for air entrainment is:

$$\frac{d}{ds}\left(\int_0^{b\sqrt{2}} \rho \cdot u \cdot 2 \cdot \pi \cdot dr\right) \tag{6}$$

$$= 2 \cdot \pi \cdot b \cdot \rho_a \cdot \left\{\alpha_1 \cdot |u^*(s)| + \alpha_2 \cdot U_a \cdot |\sin(\theta)| \cos(\theta) + \alpha_3 \cdot u'\right\}$$

where: α_1 = entrainment coefficient for a free jet, 0.057

α_2 = entrainment coefficient for a line thermal, 0.5

α_3 = entrainment coefficient due to turbulence, 1.0

u' = turbulent entrainment velocity (root mean square of the wind velocity fluctuation is used for this number), m/s

Step 4: The equations of conservation of mass, momentum, and energy are given as:

$$\frac{d}{ds}\left(\int_0^{b\sqrt{2}} c \cdot u \cdot 2 \cdot \pi \cdot dr\right) = 0 \tag{7}$$

$$\frac{d}{ds}\left(\int_0^{b\sqrt{2}} \left(\rho \cdot u^2 \cdot \cos(\theta) \cdot 2 \cdot \pi \cdot dr\right)\right) \tag{8}$$

$$= 2 \cdot \pi \cdot b \cdot \rho_a \cdot \left\{\alpha_1 \cdot |u^*(s)| + \alpha_2 \cdot U_a \cdot |\sin(\theta)| \cdot \cos(\theta) + \alpha_3 \cdot u'\right\}$$

$$+ C_d \cdot \pi \cdot b \cdot \rho_a \cdot U_a^2 |\sin(\theta)|$$

$$\frac{d}{ds}\left(\int_0^{b\sqrt{2}} \rho \cdot u^2 \cdot \cos(\theta) \cdot 2 \cdot \pi \cdot dr \right) \tag{9}$$

$$= \int_0^{b\sqrt{2}} g \cdot \left(\rho_a - \rho \right) \pi \cdot r \cdot dr \pm C_d \cdot \pi \cdot b \cdot \rho_a \cdot U_a^2 \cdot \sin(\theta) \cdot \cos(\theta)$$

$$\frac{d}{ds}\left(\int_0^{b\sqrt{2}} \rho \cdot u \left(\frac{1}{\rho} - \frac{1}{\rho_{a0}} \right) \cdot 2 \cdot \pi \cdot r \cdot dr \right) \tag{10}$$

$$= \rho_a \cdot 2 \cdot \pi \cdot b \left(\frac{1}{\rho_a} - \frac{1}{\rho_{a0}} \right) \cdot \left\{ \alpha_1 \cdot |u^*(s)| + \alpha_2 \cdot U_a \, \sin(\theta) | \cdot \cos(\theta) + \alpha_3 \cdot \dot{u} \right\}$$

The subscript 0 refers to conditions at the point of release. These equations are integrated along the path of the plume to yield the concentration profiles as a function of elevation and distance downwind of the release.

Step 5: After the steady-state equations are solved, an along-wind dispersion correction is applied to account for short-duration releases. This is accomplished using the method outlined by Palazzi, et al. [1982].

Step 6: If the plume reaches the ground, it is coupled to the Heavy Gas Dispersion Model (described in Section G) and the dispersion calculations continue.

Validation

The Momentum Jet Dispersion Model used in **CANARY** was validated by comparing results obtained from the model with experimental data from field tests. Data used for this comparison and the conditions used in the model were taken from an American Petroleum Institute (API) study [Hanna, Strimaitis, and Chang, 1991]. For this model, comparisons were made with the Desert Tortoise, Goldfish, and Prairie Grass series of dispersion tests. Results of these comparisons are shown in Figure F-1.

References

Astleford, W. J., T. B. Morrow, and J. C. Buckingham, *Hazardous Chemical Vapor Handbook for Marine Tank Vessels* (Final Report – Phase II). U.S. Coast Guard Report No. CG-D-12-83, April, 1983.

Hanna, S. R., D. G. Strimaitis, and J. C. Chang, *Hazard Response Modeling Uncertainty (A Quantitative Method), Evaluation of Commonly Used Hazardous Gas Dispersion Models*, Volume II. Study co-sponsored by the Air Force Engineering and Services Center, Tyndall Air Force Base, Florida, and the American Petroleum Institute; performed by Sigma Research Corporation, Westford, Massachusetts, September, 1991.

Havens, J., and T. Spicer, *LNG Vapor Dispersion Prediction with the DEGADIS Dense Gas Dispersion Model*. Gas Research Institute Contract No. 5086-252-1287 with the University of Arkansas, September, 1990: pp. 37-48.

Ooms, G., "A New Method for the Calculation of the Plume Path of Gases Emitted by a Stack." *Atmospheric Environment*, Vol. 6, 1972: pp. 889-909.
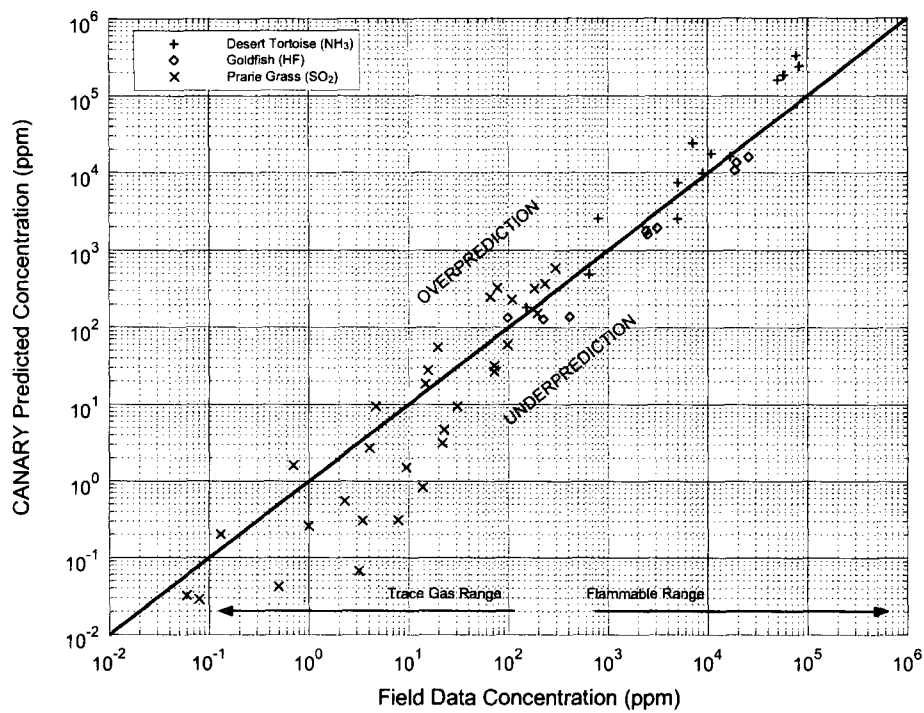
Figure F-1

Ooms, G., A. P. Mahieu, and F. Zelis, "The Plume Path of Vent Gases Heavier than Air." *First International Symposium on Loss Prevention and Safety Promotion in the Process Industries*, C. H. Buschman, Editor, Elsevier Press, 1974.

Palazzi, E., M. De Faveri, G. Fumarola, and G. Ferraiolo, "Diffusion from a Steady Source of Short Duration." *Atmospheric Environment*, Vol. 16, No. 12, 1982: pp. 2785-2790.

Heavy Gas Dispersion Model

Purpose

The purpose of this model is to predict the dispersion and gravity flow of a heavy gas released into the air from liquid pools or instantaneous gas releases. It is used to predict the downwind travel of a flammable or toxic vapor cloud.

Required Data

(a)   Composition and properties of the released material
(b)   Temperature of released material
(c)   Vapor generation rate
(d)   Vapor source area
(e)   Vapor source duration
(f)   Ambient wind speed
(g)   Ambient Pasquill-Gifford atmospheric stability class
(h)   Ambient temperature
(i)   Relative humidity
(j)   Surface roughness scale

Methodology

Step 1: For a steady-state plume, released from a stationary source, the Heavy Gas Dispersion Model solves the following equations:

$$\frac{d}{dx}\left(\rho \cdot U \cdot B \cdot h \cdot m\right) = \rho_s \cdot W_s \cdot B_s \tag{1}$$

$$\frac{d}{dx}\left(\rho \cdot U \cdot B \cdot h\right) = \rho_a \cdot \left(V_e \cdot h + W_e \cdot B\right) + \rho_s \cdot W_s \cdot B_s \tag{2}$$

$$\frac{d}{dx}\left(\rho \cdot U \cdot B \cdot h \cdot C_p \cdot T\right) = \rho_a \cdot \left(V_e \cdot h + W_e \cdot B\right) \cdot C_{pa} \cdot T_a + \rho_s \cdot W_s \cdot B_s \cdot C_{ps} \cdot T_s + f_t \tag{3}$$

$$\frac{d}{dx}\left(\rho \cdot U \cdot B \cdot h \cdot U\right)$$

$$= -0.5 \cdot \alpha_g \cdot g \cdot \frac{d}{dx}\left[\left(\rho - \rho_a\right) \cdot B \cdot h^2\right] + \rho_a \cdot \left(V_e \cdot h + W_e \cdot B\right) \cdot U_a + f_u \tag{4}$$

$$\frac{d}{dx}\left(\rho \cdot U \cdot B \cdot h \cdot V_g\right) = g \cdot \left(\rho - \rho_a\right) \cdot h^2 + f_{vg} \tag{5}$$

$$U \cdot \frac{dZ_c}{dx} = -V_g \cdot \frac{Z_c}{B} \tag{6}$$

$$U \cdot \frac{dB}{dx} = \frac{\rho_a}{\rho} \cdot V_e + V_g \tag{7}$$

$$\rho \cdot T = \frac{\rho_a \cdot T_a \cdot M_s}{\left[M_s + (M_a - M_s) \cdot m \right]} \tag{8}$$

where: x = downwind distance, m

ρ = density, kg/m^3

U = velocity in the direction of the wind, m/s

B = cloud width parameter, m

h = cloud height parameter, m

m = mass fraction of source gas

T = temperature, K

C_p = specific heat, J/(kg $\cdot$ K)

f_t = ground heat flux, J/(m$\cdot$s)

f_u = downwind friction term, kg/s^2

f_v = crosswind friction term, kg/s^2

V_e = horizontal entrainment rate, m/s

V_g = horizontal crosswind gravity flow velocity, m/s

W_e = vertical entrainment rate, m/s

W_s = vertical source gas injection velocity, m/s

M = molecular weight, kg/kmole

s = refers to source properties

a = refers to ambient properties

The first six equations are crosswind-averaged conservation equations. Equation (7) is the width equation, and Equation (8) is the equation of state.

Step 2: All of the gas cloud properties are crosswind averaged. The three-dimensional concentration distribution is calculated from the average mass concentration by assuming the following concentration profile:

$$C(x,y,z) = C(x) \cdot C_1(y) \cdot C_2(z) \tag{9}$$

$$C(x) = \frac{M_a \cdot m(x)}{M_s + (M_a - M_s) \cdot m(x)} \tag{10}$$

$$C_1(y) = \frac{1}{4 \cdot b} \cdot \left\{ erf\left(\frac{y+b}{2 \cdot \beta}\right) - erf\left(\frac{y-b}{2 \cdot \beta}\right) \right\} \tag{11}$$

$$B^2 = b^2 + 3 \cdot \beta^2 \tag{12}$$

$$C_2(z) = \left(\frac{6}{\pi}\right)^{1/2} \cdot \frac{1}{h} \cdot \exp\left(\frac{-3 \cdot z^2}{2 \cdot h^2}\right) \tag{13}$$

where: $C(x,y,z)$ = concentration in plume at x, y, z, kg/m^3
    y = crosswind coordinate, m
    z = vertical coordinate, m
    b, B, β = half-width parameters, m

Step 3: As there are now two parameters used to define $C_1(y)$, the following equation is needed to calculate b:

$$U \cdot \left(\frac{db}{dx}\right) = V_g \cdot \frac{b}{B} \tag{14}$$

Step 4: The vertical entrainment rate is defined to be:

$$W_e = \frac{\sqrt{3} \cdot a \cdot k \cdot U_* \cdot \delta\left(\dfrac{h}{H}\right)}{\Phi_h\left(\dfrac{h}{L}\right)} \tag{15}$$

where: a = constant, 1.5
    k = constant, 0.41
    U_* = friction velocity, m/s
    L = Monin-Obukhov length derived from the atmospheric stability class

Step 5: The profile function δ is used to account for the height of the mixing layer, H, and to restrict the growth of the cloud height to that of the mixing layer. H is a function of stability class and is defined as:

$$\delta\left(\frac{h}{H}\right) = 1 - \frac{h}{H} \tag{16}$$

The Monin-Obukhov function, Φ_h, is defined by:

$$\Phi_h\left(\frac{h}{L}\right) = \begin{cases} 1 + 5 \cdot \dfrac{h}{L} & L \geq 0 \text{ (stable)} \\[2ex] \left[1 - 16 \cdot \dfrac{h}{L}\right]^{-1/2} & L < 0 \text{ (unstable)} \end{cases} \tag{17}$$

Step 6: After the steady-state equations are solved, an along-wind dispersion correction is applied to account for short-duration releases. This is accomplished using the method outlined by Palazzi, et al. [1982].

Validation

The Heavy Gas Dispersion Model used in **CANARY** was validated by comparing results obtained from the model with experimental data from field tests. Data used for this comparison and the conditions used in the model were taken from an American Petroleum Institute (API) study [Hanna, Strimaitis, and Chang, 1991]. For this model, comparisons were made with the Burro, Maplin Sands, and Coyote series of dispersion tests. Results of these comparisons are shown in Figure G-1.
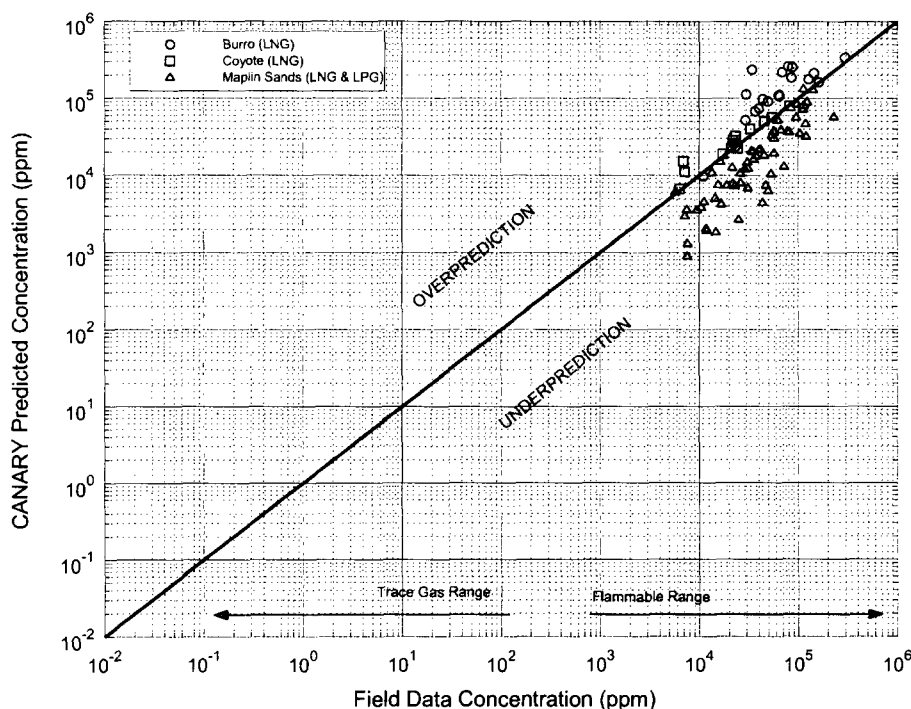

Figure G-1

References

Ermak, D. L., and S. T. Chan, *A Study of Heavy Gas Effects on the Atmospheric Dispersion of Dense Gases.* UCRL-92494, Lawrence Livermore National Laboratory, Livermore, California. Presented at the 15th NATO/CCMS International Technical Meeting on Air Pollution Modeling and Its Applications, St. Louis, Missouri, April 15-19, 1985.

Ermak, D. L., S. T. Chan, D. L. Morgan, Jr., and L. K. Morris, "A Comparison of Dense Gas Dispersion Model Simulations with Burro Series LNG Spill Test Results." *Journal of Hazardous Materials*, Vol. 6, 1982: pp. 129-160.

Ermak, D. L., and S. T. Chan, *Recent Developments on the FEM3 and SLAB Atmospheric Dispersion Models.* UCRL-94071, Lawrence Livermore National Laboratory, Livermore, California. Presented at the IMA Conference on Stably Stratified Flows and Dense Gas Dispersion, Chester, England, April 9-10, 1986.

Hanna, S. R., D. G. Strimaitis, and J. C. Chang, *Hazard Response Modeling Uncertainty (A Quantitative Method), Evaluation of Commonly-Used Hazardous Gas Dispersion Models*, Volume II. Study

cosponsored by the Air Force Engineering and Services Center, Tyndall Air Force Base, Florida, and the American Petroleum Institute; performed by Sigma Research Corporation, Westford, Massachusetts, September, 1991.

Morgan, D. L., L. K. Morris, S. T. Chan, D. L. Ermak, T. G. McRae, R. T. Cederwall, R. P. Kooperman, H. C. Goldwire, Jr., J. W. McClure, and W. J. Hogan, *Phenomenology and Modeling of Liquefied Natural Gas Vapor Dispersion.* UCRL-53581, Lawrence Livermore National Laboratory, Livermore, California, 1982.

Morgan, D. L., Jr., L. K. Morris, and D. L. Ermak, *SLAB: A Time-Dependent Computer Model for the Dispersion of Heavy Gases Released in the Atmosphere.* UCRL-53383, Lawrence Livermore National Laboratory, Livermore, California, 1983.

Palazzi, E., M. De Faveri, G. Fumarola, and G. Ferraiolo, "Diffusion from a Steady Source of Short Duration." *Atmospheric Environment*, Vol. 16, No. 12, 1982: pp. 2785-2790.